IL-33 and ST2 mediate FAK-dependent antitumor immune evasion through transcriptional networks

One-sentence summary: The kinase FAK coordinates chromatin modifiers and transcription factors to orchestrate evasion of antitumor immune responses.

Editor's summary:
FAK directs tumor immune evasion
Tumors are adept at escaping the immune system's surveillance or suppressing its activity. The kinase FAK is implicated in immune escape mechanisms. Serrels *et al*. found that FAK activates a transcriptional network that induces—and is then further mediated by—the nuclear abundance of interleukin 33 (IL-33) in tumor cells. In a mouse model of squamous cell carcinoma, FAK–IL-33 complexes boosted the production and secretion of two key factors in immunosuppression: the chemokine CCL5, which stimulates immunosuppressive regulatory T cells, and soluble ST2, a decoy receptor for cytotoxic T cell–stimulatory IL-33. Blocking these FAK-mediated signals may help the patient's immune system find and kill tumors.

IL-33 and ST2 mediate FAK-dependent antitumor immune evasion through transcriptional networks

Bryan Serrels[1*#], Niamh McGivern[1#], Marta Canel[2], Adam Byron[1], Sarah C Johnson[3], Henry Mcsorley[2], Niall Quinn[1], David Taggart[2], Alex Von Kreigsheim[1], Stephen M Anderton[2], Alan Serrels[1,2,*], Margaret C Frame[1*].

[1]Cancer Research UK Edinburgh Centre, Institute of Genetics and Molecular Medicine, University of Edinburgh, Edinburgh EH4 2XR, UK.
[2]MRC Centre for Inflammation Research, The Queen's Medical Research Institute, University of Edinburgh, Edinburgh EH16 4TJ, UK.
[3]Barts Cancer Institute, Queen Mary University of London, Charterhouse Square, London EC1M 6BQ, UK.
*Corresponding author. Email: m.frame@ed.ac.uk (M.F.), b.serrels@ed.ac.uk (B.S.), a.serrels@ed.ac.uk (A.S.).
[#]These authors contributed equally.

Abstract

Focal adhesion kinase (FAK) mediates tumor cell–intrinsic behaviors that promote tumor growth and metastasis. We previously showed that FAK also induces the expression of inflammatory genes that inhibit antitumor immunity in the microenvironment. Here, we identified a crucial, previously unknown role for the dual-function cytokine IL-33 in FAK-dependent immune evasion. In murine squamous cell carcinoma (SCC) cells, specifically nuclear FAK enhanced the expression of the genes encoding IL-33, the chemokine CCL5, and the soluble, secreted form of the IL-33 receptor sST2. The abundance of IL-33 and CCL5 was increased in FAK-positive SCC cells but not in normal keratinocytes. IL-33 associated with FAK in the nucleus, and the FAK–IL-33 complex interacted with a network of chromatin modifiers and transcriptional regulators, including TAF9, WDR82 and BRD4, which promote the activity of nuclear factor κB (NF-κB) and its induction of genes encoding chemokines,

including CCL5. We did not detect secretion of IL-33 from FAK-positive SCC cells; thus, we propose that the increased production and secretion of sST2 likely sequesters IL-33 secreted by other cell types within the tumor environment, thus blocking its stimulatory effects on infiltrating host immune cells. Depleting FAK, IL-33, or sST2 from SCC cells before implantation induced tumor regression in syngeneic mice, except when $CD8^+$ T cells were co-depleted. Our data provide mechanistic insight into how FAK controls the tumour immune environment, namely through a transcriptional regulatory network mediated by nuclear IL-33. Targeting this axis may boost antitumor immunity in patients.

Introduction

Reprogramming the immuno-suppressive tumor environment to promote anti-tumor immunity is a major objective of immuno-modulatory therapies currently in clinical use or development. Cancer cells contribute to orchestrating the composition of this environment through driving enrichment of immune cell populations with intrinsic immuno-suppressive function, thereby evading the anti-tumor activity of cytotoxic CD8 T-cells. Identification and characterization of key molecular pathways that regulate cancer cell expression of immune modulators, such as chemokines and cytokines, may therefore provide new therapeutic strategies for use in combination immunotherapy.

Focal Adhesion Kinase (FAK) is a non-receptor tyrosine kinase that signals downstream of integrins and growth factor receptors to control the malignant phenotype in multiple ways, including by regulating adhesion, migration, proliferation, and survival (*1*). FAK is frequently increased in abundance in human cancers (*2-4*), and contributes to skin, mammary, intestinal and prostate tumorigenesis in mouse models (*5-8*). A number of small-molecule FAK kinase inhibitors are now in early-

phase clinical trials. In addition to its role at the plasma membrane, FAK can also translocate to the nucleus where it can regulate gene expression (*9-11*). In a mouse model of skin squamous cell carcinoma (SCC) (*12*), we demonstrated that nuclear FAK controls expression of chemokines and cytokines, including *Ccl5* and *Tgfb2*, that drive increased numbers of regulatory T (T_{reg}) cells in the tumor environment, resulting in protection from an anti-tumor $CD8^+$ T-cell response (*9*).

IL33 is a member of the IL1 family of cytokines and is secreted by necrotic epithelial cells and activated innate immune cells, or held within the cell as a nuclear factor. Secreted IL33 binds to its cognate receptor, a heterodimeric complex comprised of ST2L (IL1RL1) and IL-1 receptor accessory protein (IL-1RAcP), to initiate activation of mitogen-activated protein kinase (MAPK) and nuclear factor -κB (NF-κB) (*13*), wherein IL33 has potent pro-inflammatory functions and is considered a "danger" signal. IL33 released into the tumor environment has been suggested to both inhibit (*14*) and promote tumor formation (*15*), indicating that IL33's roles in cancer development and progression are unclear. IL33 can also localize to the nucleus, where it either activates or represses transcription through association with the transcription factor NF-κB or the NF-κB p65 promoter, respectively (*16, 17*). The precise mechanisms that underpin IL33's regulation of transcription are not well understood.

ST2, a component of the IL33 receptor complex, can exist as a functional transmembrane receptor (ST2L) or as a shorter secreted decoy receptor (sST2) (*13*). ST2L is present on the cell surface of several hematopoietic cells, including T cells, macrophages, neutrophils and MDSCs, and activation of downstream signaling can alter cytokine production or immunosuppressive capacity (*14, 18*). ST2L of host immune cells is required for tumor clearance; hence, it has been linked to the anti-tumor properties of IL33 (*14*). Conversely, soluble ST2 (sST2) is proposed to function

as a decoy receptor for IL33, suppressing its potent pro-inflammatory functions, and high serum levels of sST2 have been correlated with poor prognosis in estrogen receptor (ER)-positive breast cancer (*19*). Like IL33, the precise role of sST2 in cancer remains somewhat controversial.

Here we found that nuclear FAK critical for the expression of *IL33* and *ST2* in cancer cells. IL33 was restricted to the nucleus in murine SCC cells, where it acts downstream of FAK to promote *Ccl5* expression and tumor growth. Mechanistic protein network analyses suggested that IL33 regulates gene expression by interacting with chromatin modifiers and transcriptional regulators. ST2 was secreted by SCC cells, and it suppressed $CD8^+$ T cell-mediated tumor clearance. Our findings reveal new insight into the molecular mechanisms by which nuclear FAK regulates chemokine expression, placing nuclear IL33 at the heart of a complex transcriptional network that specifies the anti-tumor immune response.

Results

Nuclear FAK regulates expression of IL33 and its receptor ST2.

We have previously reported that nuclear FAK regulates the expression of chemokines, including *Ccl5*, and this is important for driving infiltration of regulatory T (T_{reg}) cells into murine SCC tumors, enabling them to evade the anti-tumor immune response (*9*). To explore the mechanisms of FAK-dependent chemokine regulation, we analysed Affymetrix microarray data comparing murine *FAK*$^{-/-}$ SCC cells, with those re-expressing FAK-wt (herein referred to as FAK-wt) to identify genes that are regulated by FAK. In the set of genes significantly downregulated after FAK depletion, the only significantly enriched gene ontology term was “extracellular region” ($p = 0.049$). Using the genes contained within this category, we generated a protein

interaction network based on direct physical interactions. The largest connected network was found to contain *Ccl5* and the gene encoding the cytokine *IL33* (Fig.1A). Given the link between IL33 and the regulation of gene expression (*16, 17*), we investigated whether, and if so how, IL33 contributed to FAK-dependent transcription of chemokines.

We first used q(RT)-PCR to compare *IL33* expression in SCC cells expressing FAK-wt, *FAK*$^{-/-}$, FAK-nls (a mutant that is largely excluded from the nucleus), and FAK-kd (a kinase deficient mutant), and found that regulation of *IL33* mRNA was dependent on both FAK kinase activity and its nuclear localisation (Fig. 1B). Western blotting for IL33 abundance in whole cell lysates revealed similar findings at the protein level (Fig. 1C and fig. S1A). We have shown previously that mutation of the nuclear localization signal in FAK does not completely abolish FAK nuclear localization. We believe this explains why we observed slightly increased abundance of IL33 in cells expressing this mutant when compared to *FAK*$^{-/-}$ or FAK-kd SCC cells. Similarly, analysis of SCC cells expressing FAK-Y397F, an autophosphorylation-defective mutant of FAK that is kinase deficient, showed reduced *IL33* expression similar to that observed in *FAK*$^{-/-}$ SCC cells (fig. S1B). Treatment of FAK-wt cells with the FAK catalytic inhibitor VS4718 inhibited IL33 abundance on both mRNA and protein levels (Fig. 1, D and E), even with a low (50 nM) concentration of VS4718 (fig. S1, C and D). IL33 can function both as a nuclear cytokine and a secreted alarmin (*20*). Using both an anti-IL33 ELISA (Fig. 1F) and Western blotting (fig. S1E), we could not detect IL33 in SCC cell-conditioned media, implying that IL33 predominantly functions as a nuclear cytokine in SCC cells.

As an extracellular cytokine, IL33 mediates signalling by binding to the IL-33R complex, comprised of ST2 (also termed interleukin 1 receptor-like 1, IL1RL1), and

the IL-1 receptor accessory protein (IL-1RAcP) (*21*). Furthermore, both IL33 signalling, and nuclear IL33 have been shown to regulate *ST2* expression (*22, 23*). The protein encoded by *ST2* exists in two forms: (i) as ST2L, a membrane-anchored receptor that activates downstream signalling upon IL33 engagement, or (ii) as sST2, a secreted soluble decoy receptor that inhibits IL33 signalling (*13*). Using q(RT)-PCR with a primer set that would detect cumulative amounts of mRNA encoding both ST2L and sST2, we found that *ST2* expression was greater in FAK-wt cells when compared to *FAK*$^{-/-}$, FAK-nls, or FAK-kd cells (Fig. 1G). Thus, FAK's regulation of *ST2* expression is also dependent on both nuclear localization and kinase activity. Using an anti-ST2 ELISA, we found abundant secreted amounts of sST2 in FAK-wt cell-conditioned medium, and this was reduced in media conditioned by *FAK*$^{-/-}$, FAK-nls, and FAK-kd cells (Fig. 1H). However, flow cytometry analysis did not detect the presence of ST2L on the surface of FAK-wt and *FAK*$^{-/-}$ SCC cells (fig. S1F), indicating that sST2 is the predominantly produced isoform upon *ST2* induction in SCC cells. Treatment with the FAK inhibitor VS4718 reduced its expression and secretion (Fig. 1, I and J). Collectively, these results indicate that the kinase activity of FAK in the nucleus is a key regulator of the abundance of both nuclear IL33 and sST2, thereby influencing both the nuclear and extracellular/alarmin functions of IL33 signaling.

We next investigated the mechanism by which FAK controls *IL33* expression and sST2 abundance in SCC cells. Using an experimentally derived nuclear FAK interactome from FAK-wt cells (*9*), we used Ingenuity Pathway Analysis (IPA) to identify direct experimentally observed relationships between nuclear FAK-interacting proteins and transcription factors that regulate the expression of *IL33* and *ST2* (obtained from Qiagen's DECODE database) (fig. S1G). This identified associations with several *IL33*- and *ST2*-regulatory transcription factors. We noticed that 4 of these

associations, RUNX1, SP1, NCOA2 and NR3C1, were linked to transcription factors associated with regulating the expression of both *IL33* and *ST2*. We know that FAK associates with SP1 (confirmed in fig. S1, H and I) and RUNX1 (*24*) and is involved in regulating RUNX1-containing protein complexes, posttranslational modification, and ultimately transcription factor function. Small interfering RNA (siRNA)-mediated depletion of both RUNX1 and SP1 suggested that these transcription factors acted together to regulate IL33 abundance (fig. S1, J and K). The precise details of their coordinated activities require further investigation, but nonetheless our findings identify several connections between FAK-interacting proteins and transcription factors that regulate *IL33* and *ST2*.

IL33 is required for FAK-dependent expression of a subset of chemokines.

Nuclear IL33 has been linked to regulation of gene expression in several model systems (*16, 17*). To determine whether nuclear IL33 was required for FAK-dependent chemokine expression, we depleted IL33 in FAK-wt SCC cells using both short hairpin RNA (shRNA) (Fig. 2, A and B, and fig. S2A) and CRISPR/Cas9 (fig. S2B). IL33 has previously been linked to the regulation of *Ccl5* (*23*), and we have shown that FAK-dependent *Ccl5* expression regulates the anti-tumor immune response (*9*). We found that *IL33* and *Ccl5* expression was increased in SCC cells when compared to primary keratinocytes (Fig. 2, C and D), correlating with nuclear FAK in SCC cells, and that IL33 was required for *Ccl5* expression in FAK-wt SCC cells (Fig. 2E and fig. S2C). A previous study in endothelial cells (*23*) demonstrated that IL33 silencing increased *sST2* expression, here we found that IL33 silencing reduced sST2 abundance (fig. S2D). Although we have used different readouts (mRNA vs protein), it is likely that the regulation of *ST2* by IL33 may be context dependent. To investigate further the

requirement for IL33 in FAK-dependent chemokine expression, we performed Nanostring PanCancer Immune profiling of FAK-wt/pLKO, *FAK*$^{-/-}$, and FAK-wt/IL33-shRNA cells. Hierarchical clustering of log-transformed fold changes, relative to control cells, identified a subset of chemokines co-regulated by FAK and IL33 (Fig. 2F), including CCL5. Furthermore, overexpression of IL33 in *FAK*$^{-/-}$ SCC cells increased *Ccl5* expression (Fig. 2G), suggesting IL33 is sufficient to promote *Ccl5* expression. Therefore, FAK regulates IL33, which in turn can mediate FAK-dependent chemokine expression.

IL33/ST2 axis supports tumor growth by suppressing the immune response.

IL33 is expressed by several cell types within the tumour environment, and secreted IL33 can have both pro and anti-tumour effects (*14, 15*). ST2L, the IL33 receptor, is present on various immune cells, including T_{reg} cells, macrophages, and $CD8^+$ T cells, and activation of ST2L signalling can alter their phenotype and/or function. For example, ST2L-positive T_{reg} cells exhibit a more potent immunosuppressive function than ST2L-negative T_{reg} cells (*25*), implying that IL33-ST2L signalling could enhance the suppressive activity of T_{reg} cells, thereby promoting tumor growth. In contrast, activation of ST2L on cytotoxic $CD8^+$ T cells enhances the cells' cytotoxic function (*18*), resulting in an improved anti-tumor immune response. Therefore, it is possible that FAK-dependent regulation of the decoy receptor sST2 could have pro- or anti-tumor effects.

Having established that nuclear IL33 regulates chemokine expression, including *Ccl5*, we next assessed the effects of IL33 depletion on SCC tumor growth. Therefore, 1 x 10^6 FAK-wt, *FAK*$^{-/-}$, and FAK-wt/IL33-shRNA1 cells were injected subcutaneously into FVB mice (the syngeneic host strain), and tumor growth was

monitored. FAK-wt tumors exhibited exponential growth until they reached defined endpoints by which time the mice had to be sacrificed (see Methods section). In contrast, *FAK*$^{-/-}$ SCC tumours grew until approximately day 7, after which they stalled and underwent complete regression (Fig. 3A, left graph), as we have also reported previously (*9*). IL33 depletion from FAK-wt cells resulted in 6 out of 8 tumors exhibiting a period of growth followed by complete regression, in a similar manner to *FAK*$^{-/-}$ tumors, whereas 2 out of 8 tumours showed a growth delay (Fig. 3A). Similar studies using CRISPR/Cas9 to deplete IL33 from FAK-wt cells confirmed the requirement for IL33 in supporting SCC tumor growth (Fig. 3B). Thus, IL33 is required to support tumor growth and permit immune evasion, likely by regulating transcription of vital chemokines, including *Ccl5*.

To next probe the role of sST2 in tumor growth, we generated sST2-depleted FAK-wt SCC cell lines using shRNA (Fig. 3C) and injected 1 x 10^6 FAK-wt, FAK-wt/pLKO (shRNA control), FAK-wt/ST2-shRNA1 and FAK-wt/ST2-shRNA2 SCC cells into syngeneic FVB mice. We found that most tumours (6 out of 8 for shRNA1 and 5 out of 8 for shRNA2) exhibited a period of growth followed by complete regression (Fig. 3D), like *FAK*$^{-/-}$ tumors, albeit with different kinetics. To address how sST2 depletion might result in tumor regression, we profiled the immune cells in FAK-wt tumors to determine the quantity of ST2L on the cell surface. We found that after 12 days of growth, FAK-wt tumors have an extensive immune cell infiltrate accounting for approximately 60% of the viable cell population (Fig. 3, E and F). Using a range of surface and intracellular markers (table S1), we identified activated $CD8^+$ T cells, activated $CD4^+$ T-cells, T_{reg} cells, neutrophils, and macrophages as the major immune cell populations that displayed surface-bound ST2L (Fig. 3, G and H). Because IL33 engagement with ST2L expressed on activated $CD8^+$ T cells can enhance cytotoxic

function and drive increased expression of the effector cytokine interferon-gamma (IFNγ) (*14*), we hypothesized that tumor regression in response to depletion of sST2 from SCC cancer cells was likely $CD8^+$ T-cell dependent. To test this, we used CD8-depleting antibodies and found that depletion of $CD8^+$ T cells was sufficient to completely rescue the growth of FAK-wt/ST2-shRNA SCC tumors (Fig. 3I), implying that sST2 from the tumor cells plays an important role in supressing $CD8^+$ T cell-mediated anti-tumour immunity. Consistent with previous results (*9*), we also observed enhanced growth of FAK-wt tumors upon depletion of $CD8^+$ T cells, implying that even the FAK-wt cells remain under negative pressure from the $CD8^+$ T-cell mediated immune response.

Nuclear IL33 interacts with an extensive network of transcriptional regulators.

Having established an important role for nuclear IL33 in the regulation of chemokine expression and tumour growth, we addressed the molecular mechanisms that may underpin IL33's regulation of chemokine transcription. Using cellular fractionation, we prepared cytoplasmic, nuclear, and chromatin extracts from FAK-wt and *FAK*$^{-/-}$ SCC cells as we have done before (*9*). Our results show that IL33 is largely chromatin-associated (Fig. 4A), in agreement with previous studies that identified IL33 as a histone H2A/2B binding protein (*26*). To investigate the functional significance of IL33 association with chromatin, we made use of a proteomics technique called "BioID" (*27*). Firstly, we generated an IL33 protein fused to the 35KDa *E. coli* biotin protein ligase BirA (IL33-BirA). Next, we expressed either IL33-BirA, or BirA alone, in FAK-wt cells from which endogenous IL33 was deleted (FAK-wt/IL33-CRISPR SCC cells; Fig. 4, B and C), and cultured these in the presence of biotin for 24 hours. This resulted in the biotinylation of proximal interacting proteins, enabling their purification

and identification by mass spectrometry. To ensure identification of robust interactions, we applied stringent criteria, including that: (i) proteins must be present in all 3 biological replicates, (ii) proteins must have greater than 3-fold enrichment when compared to BirA only control, and (iii) fold enrichment must be statistically significant ($p < 0.05$). With these criteria, we identified 105 proteins that associated with IL33. Gene ontology analysis of both biological and cellular processes (DAVID bioinformatics database) represented within the dataset identified significantly enriched terms associated with chromatin organisation and transcriptional regulation (fig. S3, A and B). Further analysis of the nuclear IL33 interactome using IPA identified a connected network of proteins that were implicated in regulation of transcription, chromatin remodelling and nucleosome disassembly (Fig. 4D). There were several members of the Baf-type complex (also known as SWI/SNF), the PTW/PP1 phosphatase complex, and the transcription factor TFIID complex, establishing a novel link between nuclear IL33 and the core transcriptional machinery. We extracted a complete list of genes belonging to these complexes from the gene ontology database AmiGO, and used IPA to reconstruct all three complexes based on known physical interactions (fig. S3, C to E). We next contextualised the BioID proteomics-informed IL33 nuclear interactome onto these networks (highlighted in pink in fig. S3, C to E), and identified potential interactions linking IL33 to key members of these complexes. Using streptavidin pulldown following incubation of IL33-BirA fusion protein expressing FAK-wt/IL33-CRISPR SCC cells in the presence of biotin, we confirmed the interactions of IL33 with WDR82, SMARCC1, and TAF9 (Fig. 4E). We found that IL33 depletion in FAK-wt cells resulted in loss of WDR82 from the chromatin fraction (Fig. 4F), implying that IL33 is required to stabilize the association of WDR82 with chromatin. We find this interesting because WDR82 is a key component of complexes

associated with chromatin modification, such as the PTW/PP1 phosphatase complex (*28*) and the Set1A/Set1B histone H3-Lys^4 (H3K4) methyltransferase complex (*29*). Therefore, IL33 likely plays a key role in scaffolding complexes required to modulate chromatin structure and permit transcription.

IL33 interacts with and enhances regulators of *Ccl5* expression

As mentioned above, we previously showed that CCL5 secreted by FAK-wt SCC cells drives the infiltration of immuno-suppressive regulatory T_{reg} cells into SCC tumors, shifting the $CD8^+$ T-cell:T_{reg} ratio in favor of tumor tolerance (*9*). Thus far, we have found that IL33 is both necessary and sufficient to drive *Ccl5* expression downstream of FAK (Fig. 2, E and G). To define how IL33 contributes to regulation of *Ccl5* expression we mapped the nuclear IL33 interactome onto a network of proteins associated with predicted *Ccl5* transcription factors (Fig. 4G). This revealed that IL33 interacts with transcription factors and transcriptional regulators that impact on expression of *Ccl5*. Of note, three factors belonging to the transcription factor IID complex (TFIID) were found to interact with nuclear IL33, including TAF9, a protein we found previously to form complexes with FAK (*9*). To explore the connection between FAK, IL33, and *Ccl5* transcription, we mapped the nuclear FAK interactome onto the set of *Ccl5* regulatory proteins found to interact with nuclear IL33 (Fig. 4G). This identified proteins in common between the nuclear FAK and nuclear IL33 interactomes, suggesting that these proteins may be part of the same molecular complexes that regulate *Ccl5* expression. Using streptavidin-coated beads, we isolated the IL33 BioID fusion protein, and confirmed that FAK and IL33 exist in complex under steady state conditions (Fig. 4H). Hence, we conclude that FAK binds

to IL33, and together they complex with key *Ccl5*-regulatory transcription factors, to co-regulate chemokine gene expression.

Besides TFIID, many of the IL33 interacting partners converge on regulators of NF-κB, suggesting that NF-κB may be central to FAK and IL33s regulation of chemokine expression. Of note, we showed that IL33 interacts with the bromodomain protein BRD4, and the histone deacetylase, HDAC1 (Fig. 4H). BRD4 is a member of the bromodomain and extraterminal domain (BET) family of transcriptional coactivators and elongation factors that recruit chromatin remodelling factors, including the SWI/SNF complex (*30*), to the promoters of genes via recognition of polyacetylated histone tails (*31*). Because IL33 binds to both BRD4, and members of the Baf-type (SWI/SNF) complex, we hypothesize that IL33 plays a role in formation of this complex at actively transcribing genes. It is known that BRD4 directly binds to acetylated p65 NF-κB, which leads to enhanced NF-κB transactivation activity (*32*), together suggesting a role for BRD4 in inflammatory transcriptional signalling. To support these conclusions, we treated FAK-wt SCC cells with the BET family inhibitor JQ1. This resulted in reduced *Ccl5* expression (Fig. 4I), implying a role for BET family proteins in the regulation of chemokine expression. In contrast, HDAC1 has been shown to negatively regulate NF-κB transcriptional activity via a direct interaction with p65 (RelA) (*33*). We used the HDAC inhibitor vorinostat, and identified a clear induction of *Ccl5* expression upon HDAC inhibition (Fig. 4J). Collectively, our data support a model whereby FAK binds to IL33, which is a central component of a network of transcriptional regulators associated with the dynamic regulation of NF-κB-dependent chemokine transcription.

Discussion

Nuclear FAK is emerging as an important regulator of gene expression in cancer cells, controlling transcriptional networks that influence multiple cellular functions. For example, FAK is reported to interact with the transcription factors p53 and GATA4, resulting in their inactivation with effects on cell survival (*34*). We have shown that nuclear FAK regulates expression of chemokines and cytokines, including *Ccl5*, likely via interactions with transcription factors and transcriptional regulators (*9*). Here, we show for the first time that the both IL33 and sST2 are transcriptionally regulated by nuclear FAK in a kinase-dependent manner, and that FAK interacts with transcription factors and transcriptional regulators linked to control of expression of *IL33* and *ST2*.

Depletion of IL33 abundance in FAK-wt cells revealed that it is vital downstream of FAK in the regulation of chemokine expression, including that of *Ccl5*. We have previously identified a CCL5–CCR1/3/5 paracrine signalling axis between SCC FAK-wt cells and tumor infiltrating T_{reg} cells, and have shown that CCL5 depletion results in FAK-wt tumor regression as a result of reduced tumor infiltrating T_{reg} cells (*9*). Our tumor growth studies here revealed that IL33 depletion caused FAK-wt tumor regression, presumably due to IL33-dependent regulation of *Ccl5* and other chemokines. Thus, IL33 regulates pro-inflammatory gene programs downstream of FAK that we have shown play an important role in defining the tumour immune environment, impacting on SCC tumor growth and survival.

sST2 functions as a decoy receptor that is secreted into the tumor environment, leading to competitive inhibition of IL33-ST2 autocrine and paracrine signalling (*13*). Although IL33 is not secreted by SCC cells, it can be secreted by macrophages and neutrophils (*35*), influencing the function of immune cell populations. ST2L is also present on activated $CD8^+$ T-cells and Natural Killer (NK) cells, and IL33 stimulation

can increase IFNγ expression (*14*) and cytotoxic activity (*18*). We identified ST2L on several immune cell types in the SCC tumor environment, including activated $CD8^+$ T cells. Depletion of sST2 in FAK-wt tumors largely resulted in $CD8^+$ T cell-dependent tumor regression, implying that sST2 contributes to inhibition of $CD8^+$ T cell-mediated immunity. Studies using an *ST2* knockout mouse have shown that host ST2 signalling is required for tumor regression to occur in response to overexpression of a secreted form of IL33 (*14*). Therefore, we conclude that the presence of sST2 enables FAK-abundant tumors to benefit from nuclear IL33 while counteracting the potential anti-tumor effects of secreted IL33 (Fig. 5).

Nuclear IL33 has been linked to regulation of transcription previously (*16, 17*), although the precise mechanisms underpinning this are unknown. We confirmed that nuclear IL33 interacts with chromatin, supporting its role in transcriptional regulation, and BioID proteomics identified proximal interactions with components of the Baf-type (SWI/SNF), PTW/PP1 phosphatase and TFIID complexes. This implies that nuclear IL33 functions in chromatin remodelling and transcriptional initiation. In support of this, we confirmed binding of WDR82, SMARCC1, TAF9, BRD4, and HDAC1, and showed that WDR82 was absent from chromatin after depletion of IL33 from FAK-wt cells, showing that IL33 is required to stabilize the WDR82 chromatin complex. WDR82 is a component of the PTW/PP1 phosphatase complex and is involved in regulating chromatin structure (*28*). It is also a core component of the mammalian Set1A/Set1B histone H3K4 methyltransferase complex that is associated with regulating H3K4 tri-methylation, a key step in transcriptional activation (*36*).

Finally, we identified BRD4 and HDAC1 positive (*37*) and negative (*33*) regulators of NF-κB activity, respectively, as previously unknown nuclear IL33-interacting proteins. BRD4 is also required for recruitment of the SWI/SNF complex to

active promoters (*30*), and we have shown that IL33 binds to several components of this complex. Therefore, IL33 likely binds to BRD4, HDAC1, and other chromatin modifiers to control the dynamic expression of NF-κB-target genes, such as *Ccl5* and other chemokines. Collectively, our data suggest that IL33 acts to regulate chromatin organization and FAK-dependent transcription, promoting a pro-inflammatory gene program that enables evasion of the anti-tumor immune response.

Materials and Methods

Cell lines

Isolation and generation of the FAK SCC cell model is described in detail in Serrels *et al*. (12). Briefly, squamous cell carcinoma cells (SCCs) were induced in K14*Cre*ER $FAK^{flox/flox}$ mice on an FVB background using the DMBA/TPA two-stage skin chemical carcinogenesis protocol and cells isolated. Following treatment with 4-hydroxytamoxifen, a FAK-null ($FAK^{-/-}$) cell clone was isolated, and retroviral transduction was used to stably re-express FAK-wt and FAK mutant proteins. Phoenix Ecotropic cells were transfected with pWZL (Hygro) FAK using Lipofectamine 2000 (Thermo Scientific) according to manufacturer's instructions. Twenty-four hours post-transfection, cell culture supernatant was removed, filtered through a 0.45-μm Millex-HA filter (Millipore), diluted at a 1:1 ratio in normal SCC cell culture medium, supplemented with 5 μg/ml polybrene, and added to SCC FAK-/- cells for 24 hours. A total of two rounds of infection were performed to generate each cell line. Cells were cultured at 37°C in Glasgow minimum essential medium (MEM) (Sigma- Aldrich) supplemented with 2 mM L-glutamine, MEM vitamins, 1 mM sodium pyruvate (all Sigma-Aldrich), MEM amino acids, and 10% fetal bovine serum (FBS) (both Life Technologies), and maintained under selection using 0.25 mg/ml hygromycin. To

overexpress IL33 in *FAK*$^{-/-}$ SCC cells, the cells were transfected with 1.5 µg of IL33 pcDNA3.1 (synthesized optimized sequence by Geneart - Life Technologies) using Lipofectamine 2000. Cells were selected in 400 µg/ml of G418, and overexpression of IL33 was confirmed by Western blotting.

shRNA-mediated ST2 and IL33 Knockdown

To generate lentiviral particles, 2x10^6 HEK293FT cells were transfected with a mixture of 2 µg shRNA [RMM4534-EG77125 (IL33), RMM4534-EG17082 (ST2/IL1l1R); GE Healthcare], 0.5 µg MDG2 and 1 µg PAX2 plasmid DNA using Lipofectamine 2000 (ThermoFisher Scientific) as per manufacturers guidelines. Forty-eight hours post transfection, media was removed and filtered through a 0.45µm Millex-AC filter (Millipore) and mixed at a 1:1 ratio with normal SCC growth medium, supplemented with polybrene (Millipore) to a final concentration of 5 µg/ml, and added to SCC cells for twenty-four hours. Cells were subjected to two rounds of lentiviral infection prior to selection in 2 µg/ml of puromycin.

siRNA mediated knockdown of SP1 and RUNX1

To knockdown SP1 and RUNX1, FAK-wt SCC cells were transfected 10nmol of non-targeting siRNA Smartpool, SP1 siRNA Smartpool or Runx1 siRNA smartpool (all Dharmacon, siGenome), or a combination of 10nmol SP1 and RUNX1 siRNA Smartpool using hyperfect transfection reagent (Qiagen as per manufacturers guidelines). Transfection was performed in serum free media for 24 hours, after which the media was replaced with normal growth media. Protein lysates were collected 48 hours after transfection.

IL33 CRISPR construct generation

Guide sequence oligonucleotides (Forward: TTTCTTGGCTTTATATATCTTGTG GAAAGGACGAAACACCGTTCCTAGAATCCCGTGGAT Reverse: GACTAGCCTTA TTTTAACTTGCTATTTCTAGCTCTAAAACATCCACGGGATTCTAGGAAC) including EcoR I restriction overhangs and a PAM sequence targeting exon three within *IL33* were annealed using High Fidelity Phusion Polymerase (NEB) according to manufacturers guidelines. 10 µM of each oligonucleotide was mixed with 25mM $MgCl_2$, 2.5mM dNTP, 5x High Fidelity Phusion Buffer, and Phusion Polymerase to a final volume of 50 µl. Cycling conditions were 98ºC (30 seconds), 30 cycles of 98ºC (10 seconds), 55ºC (30 seconds) 72ºC (20 seconds), followed by a final incubation at 72ºC (20 seconds). The final PCR product was analysed by agarose gel electrophoresis. Annealed oligonucleotides were ligated into the gRNA_Cloning Vector (pCR-Blunt II-TOPO), a gift from George Church (Addgene plasmid # 41824). 1.5 µg of gRNA_cloning vector DNA was digested with 1.5 units of Aflii restriction enzyme (NEB) according to manufacturers guidelines, and incubated for 1 hour at 37ºC. 4 ng of annealed oligonucleotides were ligated with 30 ng of linearized gRNA_cloning vector using Gibson assembly master mix (New England Biolabs) according to manufacturers guidelines, and incubated for 1 hour at 50ºC. Constructs were transformed into DH5α chemically competent cells and selected on agar plates containing 50 µg/ml of kanamycin. To identify positive colonies, DNA was prepared and digested with EcoR I restriction enzyme (NEB).

IL33 CRISPR/Cas9 transfection and single cell clone expansion

SCC-FAK-wt cells were seeded on a 100mm tissue culture dish and grown until ~70% confluent. Cells were co-transfected with 3 µg of hCas9, and 3 µg of gRNA vector containing IL33 specific guides, using Lipofectamine 2000 (Thermo Scientific)

according to manufacturers guidelines. IL33 CRISPR knockout clones were isolated by dilution cloning; once cells reached confluence they were trypsinized and re-suspended in 10 mls of growth media. To ensure single cell suspension, cells were passed through a cell strainer (Thermo Scientific), and 5 µl of the cell suspension was plated into a 15cm plate. Several colonies were picked and expanded, and knockout of IL33 was confirmed by qPCR and western blot. IL33 primers used were: forward GGATCCGATTTTCGAGAGCTTAAACAT reverse: GCGGCCGCATGAGACCTAGAATGAAGT

Immunoblotting

Cells were washed twice in ice cold phosphate buffered saline (PBS) and lysed in RIPA lysis buffer (50mM Tris-HCL at pH7.4, 150mM Sodium Chloride, 5mM EGTA, 0.1% SDS, 1% NP40, 1% Deoxycholate) supplemented with a protease /phosphatase inhibitor cocktail (mini complete Ultra Protease tablet and phosSTOP tablet from Roche). Lysates were clarified by high-speed centrifugation (16,000g for 15 min at 4°C). Protein concentration was measured using a micro BCA protein assay (ThermoScientific), and 10-20 µg of total protein was supplemented with 2x SDS sample buffer (Tris pH6.8, 20% Glycerol, 5% SDS, β-mercaptoethanol, Bromo-phenol blue), and boiled at 95°C for 5 minutes. Samples were separated by polyacrylamide gel electrophoresis using 4-15% mini-protean TGX gels (BioRad), proteins transferred to nitrocellulose, blocked [5% bovine serum albumin in PBS–Tween 20 (BSA/PBS-T)], and probed with either anti-IL33 (R&D Biosystems), anti-GAPDH (Cell Signaling Technology), anti-phospho-FAK (Y397) (Cell Signaling Technology), anti-FAK (Cell Signaling), anti-WDR82 (Abcam), anti-TAF9 (Abcam), anti- SMARC C1 (Abcam), anti-BRD4 (Abcam), anti-HP1 aplha/beta (Cell Signaling Technology), anti-SP1(Abcam),

anti-Runx1 (Cell Signalling Technology), and anti-HDAC1 Abs (Cell Signalling Technology) (all 1:1000 in 5% BSA/PBS-T). Bound antibody was detected by incubation with anti-rabbit, anti-mouse or streptavidin conjugated-HRP secondary antibody (Cell Signaling Technology), and visualized using the BioRad ChemiDoc MP Imaging System.

Chromatin preparation

$1.5x10^6$ cells were plated into 100mm dishes and after twenty-four hours, washed twice in cold PBS. Cells were lysed in 400 µl of extraction buffer (10mM HEPES, pH7.9, 10mM KCl, 1.5mM $MgCl_2$, 0.34M sucrose, 10% glycerol, 0.2% NP-40 substitute) containing protease/phopshatase inhibitors (mini complete Ultra Protease tablet and phosSTOP tablet from Roche). Lysates were cleared at 6,500g for 5 minutes at 4^{o}C. The resulting nuclear pellet was washed in extraction buffer without NP-40, and centrifuged at 6,500g for 5 minutes at 4^{o}C. The pellet was re-suspended in 400 µl of no salt buffer (10mM HEPES pH7.9, 3mM EDTA, 0.2mM EGTA), incubated at 4^{o}C for 30 minutes with agitation, and centrifuged at 6500g for 5 minutes at 4^{o}C. The pellet was re-suspended in 160 µl of high salt solubilisation buffer (50mM Tris-HCl pH8.0,2.5M NaCl, 0.05% NP-40) vortexed briefly, incubated at 4^{o}C for 30 minutes with agitation, and centrifuged at 16,000g for 10 minutes at 4^{o}C. The supernatant containing chromatin fraction was collected, and TCA precipitation was performed. Tri-chloroacetic acid (TCA) was added to a final volume of 10%, and samples were incubated for 15 minutes on ice. Following centrifugation at 21,000g for 15 minutes the resulting pellet was washed twice in 500 µl of cold acetone, and then allowed to air dry. The pellet was then re-suspended in 20 µl 2x sample buffer (Tris pH6.8, 20% Glycerol, 5% SDS, β-mercaptoethanol, Bromo-phenol blue) and boiled at 75^{o}C for 10 minutes. Samples were separated by polyacrylamide gel electrophoresis on a 12%

Mini-Protean TGX gel (BioRad), transferred onto nitrocellulose membrane, blocked [5% bovine serum albumin in PBS–Tween 20 (BSA/PBS-T)], then incubated with primary and secondary antibodies as above.

sST2 and IL33 ELISA

$2x10^6$ cells were plated on a 100mm tissue culture dish and left to adhere overnight. Media was replaced with 4ml fresh complete growth media and conditioned for 24hrs, collected and spun at 1000rpm for 5mins to remove debris. Media samples were analysed for sST2 levels using a mouse ST2 Quantikine ELISA kit or mouse IL33 Quantikine Elisa kit (R and D Systems). Cells adhered to the tissue culture dish were washed 2x in ice cold PBS and lysed in RIPA lysis buffer as above. Protein concentration was measured using micro BCA protein assay and protein quantities were used for normalisation of ELISA values.

q-RT-PCR and Nanostring

RNA was prepared from cells using the Qiagen RNeasy mini kit as per manufacturer's instructions, inclusive of DNase digestion. Final concentration of RNA was measured using a Nanodrop (Thermo Scientific). For q-RT-PCR, 5 µg of total RNA was converted to cDNA using the superscript II cDNA synthesis kit (Thermo Scientific). For quantitative real-time PCR, 62.5ng of cDNA was added to SYBR Green (Applied Biosystems), supplemented with 0.25 µl of 10µM qPCR primers to a final reaction volume of 10 µl. IL33 primers used were: forward GGATCCGATTTTCGAGAGCTTAAACAT reverse: GCGGCCGCATGAGACCTAGAATGAAGT, ST2 primers used were: GCGGAGAATGGAAGCAACTA reverse: AAGCAAGCTGAACAGGCAAT, Ccl5

primers used were: forward CCCTCACCATCATCCTCACT reverse CCTTCGAGTGACAAACACGA. Quantitative real time PCR was performed on a StepOne Plus qRT-PCR instrument (Applied Biosystems). PCR conditions were as follows: 95°C (3 minutes), followed by 40 cycles of 95ºC (5 seconds), 60ºC (10 seconds), and 72ºC (10 seconds). Melt curve analysis was performed following each qPCR reaction. Data was analysed using the ddCT method, and expression calculated relative to GAPDH. For Nanostring analysis, 150ng of RNA was labelled with gene specific bar codes as per manufacturer's instructions and quantified using a Nanostring ncounter DX. Nanostring analysis was carried out by the Newcastle Nanostring ncounter analysis service. Analysis was performed using nSolver analysis software (Nanostring).

Generation of IL33-BirA expressing SCC Cell Line

IL33 cDNA was amplified by PCR using gene specific primers (Forward: GCAGCAGCGGCCGCATGAGACCTAGAATGAAGTATTCCAAC Reverse: TGCTGCGGATCCGATTTTCGAGAGCTTAAACATAATATTG), and sub-cloned into the Not1/BamH1 sites of pQCXIN-BirA-Myc. Specifically, 20ng of pcDNA-3.1 IL33 DNA template was mixed with 10 µM of each primer in PfuUltra Hotstart master mix (Stratagene) and subjected to PCR with cycle conditions as follows: 98ºC (30 seconds), 30 cycles; 98ºC (10 seconds), 60ºC (30 seconds), 72ºC (1 minute), followed by a final incubation at 72ºC (10 minutes). Following PCR, samples were gel purified (Qiagen Gel Purification Kit) and eluted in 30 µl of nuclease free water (NFW). Purified PCR product was incubated with 1 µl BamH1 restriction enzyme, 1 µl NOT1 restriction enzyme, 5 µl of Buffer 3.1(all New England Biolabs) to a total of 20 µl, and incubated at 37ºC for 2 hours. 1 µg of pQCXIN-BirA-Myc was incubated with 1 µl BamH1

restriction enzyme, 1µl NOT1 restriction enzyme, 5 µl of Buffer 3.1 to a total of 20ul and incubated at 37°C for 1 hour. Following digestion, both the PCR product and digested vector were gel purified and eluted in 30 µl of nuclease free water. To ligate the digested IL33 PCR product into the BamH1/NOT1 sites of pQCXIN-BirA-Myc, a 1:4 ratio of digested vector to PCR product was used, and incubated with 0.5 µl of T4 DNA ligase (New England Biolabs), along with DNA ligase buffer in a final reaction volume of 10ul, and incubated for 2 hours at room temperature. 50 µl of DH5alpha chemically competent cells (Life Technologies) were transformed with 5 µl of ligation reaction according to manufacturers guidelines, and plated onto agar plates containing 100 µg /ml of ampicillin. Resulting colonies were checked for successful ligation using a diagnostic digest with BamH1 and NOT1 restriction enzymes, and if positive sequenced. Phoenix Ecotropic cells were transfected with empty vector-BirA or IL33-BirA using Lipofectamine 2000 (Thermo Scientific) according to manufacturer's guidelines. Forty-eight hours post-transfection, cell culture supernatant was removed, filtered through a 0.45-µm Millex-HA filter (Millipore), diluted at a 1:1 ratio in normal SCC cell culture medium, supplemented with 5 µg/ml polybrene, and added to SCC FAK-wt IL33-CRISPR cells for 24 hours. A total of two rounds of infection were performed to generate each cell line prior to selection in 400 µg /ml of G418.

Proteomic analysis of the IL33 interactome using BioID

Cells were incubated with 50 µM biotin (Sigma Aldridge) in complete cell culture medium at 37°C for 24hrs, washed 2x in ice cold PBS, and lysed in RIPA lysis buffer as above. Cell lysates were sonicated using a Bioruptor (Diagenode), 30 second pulses with 30 second intervals over 5mins, and cleared by high speed centrifugation (16,000g for 15min at 4°C). Protein concentration was measured using a micro BCA

protein assay (Thermo Scientific) and 1 mg of total cell lysate was incubated with 50 µl of streptavidin-C1 dynabeads (Life Technologies) overnight at 4°C with agitation. Beads were washed using a magnetic tube rack 3x with ice cold RIPA buffer and 2x with ice cold PBS. Captured proteins (from experiments performed in biological triplicate) were subjected to on-bead proteolytic digestion, desalting and liquid chromatography-tandem mass spectrometry as described previously (*38*). Mean label-free MS intensities were calculated for each biological replicate. Peptide and protein false discovery rates were set to 1%. Proteins enriched from SCC-FAK-wt lL33-CRSIPR-IL33-BirA cells by at least 3-fold when compared to SCC-FAK-wt IL33-CRISPR-EV-BirA ($p<0.05$) were considered specific. Proteomics analysis of nuclear FAK protein complexes is described in (*9*). All other protein interaction network analysis was performed using Ingenuity Pathway Analysis (Qiagen). The IL33 mass spectrometery proteomics data have been deposited to the ProteomeXchange Consortium via the PRIDE partner repository (*39*) with the dataset identifier PXD007698.

Interaction network analysis

Genes differentially expressed in *FAK*$^{-/-}$ SCC cells compared to FAK-wt SCC cells were extracted from microarray data (*9*) using rank product analysis. Significantly differentially expressed genes ($p < 0.0005$, percentage false positives (*pfp)* < 0.05) were subjected to gene ontology enrichment analysis using DAVID Bioinformatics Resources (version 6.8) (*40*).Genes annotated with overrepresented top-level cellular component terms as determined by Benjamini–Hochberg-corrected hypergeometric test ($p < 0.05$) were used to seed a protein interaction network based on direct physical interactions constructed using the GeneMANIA plugin (version 3.4.1; mouse

interactions) in Cytoscape (version 3.3.0) (*41*). The largest connected graph component was clustered using the Allegro Spring-Electric force-directed algorithm (AllegroViva).

Hierarchical cluster analysis

Unsupervised agglomerative hierarchical clustering was performed on the basis on Euclidean distance or Pearson correlation computed with an average-linkage or complete-linkage matrix using R or Cluster 3.0 (C Clustering Library, version 1.50) (*42*). Clustering results were visualised using R or Java TreeView (version 1.1.6) (*43*) and MultiExperiment Viewer (version 4.8.1) (*44*).

Inhibitor treatment

FAK-wt SCC cells were treated with doses ranging from 50-250nM VS4718 for 24 hours, 10 μM vorinostat for 24 hours, or 200 nM JQ1 for 48 hours, after which RNA or protein lysates were collected for q-RT-PCR or western blot analysis as described above. All inhibitors were obtained from Selleckchem.

Subcutaneous tumour growth

All experiments involving animals were carried out in accordance with the UK Coordinating Committee on Cancer Research guidelines by approved protocol (Home Office Project License no. 60/4248). $1x10^6$ cells SCC cells (defined earlier) were injected into both flanks of FVB mice and tumour growth was measured twice-weekly using calipers. Animals were sacrificed by cervical dislocation when tumours reached maximum allowed size (1.5cm diameter) or when signs of ulceration were evident. Group sizes ranged from 3-5 mice, each bearing two tumours, and tumour volume

was calculated in Excel (Microsoft) using formula $x\text{-}4/3\pi r^3$. Statistics and graphs were calculated using Prism (GraphPad).

CD8+T-cell Depletion

Anti-mouse CD8 (clone 53-6.7) and appropriate isotype control Abs (Rat IgG2a) were purchased from BioXcel. T-cell depletion was achieved following intra-peritoneal (IP) injection of 150 µg of depleting antibody (same for all antibodies) into female age-matched FVB mice for 3 consecutive days, and maintained by further IP injection at 7-day intervals until the study was terminated. 1 x 10^6 SCC FAK-wt or FAK-/- cells were injected subcutaneously into both flanks 6 days after initial antibody treatment, and tumor growth was measured twice-weekly as described above.

FACS Analysis of Immune Cell Populations

Tumors established following injection of 1 x 10^6 SCC cells into both flanks of FVB mice were removed at day 12 into RPMI (Sigma-Aldrich) supplemented with 10% FBS (Life Technologies). Tumor tissue was mashed into a pulp using a scalpel and re-suspended in DMEM (Sigma-Aldrich) supplemented with 2 mg/ml collagenase D and DNase1 (200U/ml) (Roche). Samples were incubated for 30 mins at 37°C with agitation, pelleted by centrifugation at 1600 rpm for 5 min at 4°C, resuspended in 5 ml of red blood cell lysis buffer (Pharm Lysis Buffer, Becton Dickinson) for 10 min at 37°C, pelleted by centrifugation at 1600 rpm for 5 min at 4°C, re-suspended in PBS and mashed through a 70-µm cell strainer. The resulting single cell suspension pellet was pelleted by centrifugation at 1600 rpm for 5 min at 4°C and re-suspended in PBS. This step was repeated a further time and the resulting cell pellets resuspended in 100 µl PBS containing e506 fixable viability dye (1/1000 dilution) and transferred into the well

of a round bottom 96-well plate. Samples were incubated at 4°C for 30 minutes. Cells were then pelleted by centrifugation at 1600 rpm for 5 min at 4°C and re-suspended in FACS buffer (PBS containing 1% FBS and 0.1% sodium azide). This step was repeated a total of three times. Cell pellets were re-suspended in 100 µl of Fc block (1:200 dilution of Fc antibody (eBioscience) in FACS buffer) and incubated for 15 min at room temperature (RT). 100 µl of antibody mixture (1:200 dilution of antibodies except anti-FoxP3 which was used at 1:100 (listed in fig. S3) in FACS buffer) were added to each well and the samples incubated for 30 min in the dark at 4°C. The plate was then centrifuged at 1600 rpm for 5 min at 4°C and the cells re-suspended in FACS buffer. This step was repeated 3 times. Samples were analyzed using a BD Fortessa FACS Analyser. Data analysis was performed using FlowJo software. All antibodies were from eBioscience. Statistics and graphs were calculated using Prism (GraphPad).

Supplementary Materials

Figure S1. Identification of common upstream regulators of *IL33* and *ST2* promoter-associated transcription factors.

Figure S2. CRIPSR knockout of *IL33* reduces *Ccl5* expression.

Figure S3. Gene Ontology enrichment analysis.

Table S1. Immune cell population markers.

Table S2. Primer sequences.

References and Notes

1. F. J. Sulzmaier, C. Jean, D. D. Schlaepfer, FAK in cancer: mechanistic findings and clinical applications. *Nat Rev Cancer* **14**, 598-610 (2014).
2. H. M. Lightfoot, Jr., A. Lark, C. A. Livasy, D. T. Moore, D. Cowan, L. Dressler, R. J. Craven, W. G. Cance, Upregulation of focal adhesion kinase (FAK) expression in ductal carcinoma in situ (DCIS) is an early event in breast tumorigenesis. *Breast Cancer Res Treat* **88**, 109-116 (2004).
3. A. L. Lark, C. A. Livasy, B. Calvo, L. Caskey, D. T. Moore, X. Yang, W. G. Cance, Overexpression of focal adhesion kinase in primary colorectal carcinomas and colorectal liver metastases: immunohistochemistry and real-time PCR analyses. *Clin Cancer Res* **9**, 215-222 (2003).
4. M. Agochiya, V. G. Brunton, D. W. Owens, E. K. Parkinson, C. Paraskeva, W. N. Keith, M. C. Frame, Increased dosage and amplification of the focal adhesion kinase gene in human cancer cells. *Oncogene* **18**, 5646-5653 (1999).
5. G. W. McLean, N. H. Komiyama, B. Serrels, H. Asano, L. Reynolds, F. Conti, K. Hodivala-Dilke, D. Metzger, P. Chambon, S. G. Grant, M. C. Frame, Specific deletion of focal adhesion kinase suppresses tumor formation and blocks malignant progression. *Genes Dev* **18**, 2998-3003 (2004).
6. H. Lahlou, V. Sanguin-Gendreau, D. Zuo, R. D. Cardiff, G. W. McLean, M. C. Frame, W. J. Muller, Mammary epithelial-specific disruption of the focal adhesion kinase blocks mammary tumor progression. *Proc Natl Acad Sci U S A* **104**, 20302-20307 (2007).
7. G. H. Ashton, J. P. Morton, K. Myant, T. J. Phesse, R. A. Ridgway, V. Marsh, J. A. Wilkins, D. Athineos, V. Muncan, R. Kemp, K. Neufeld, H. Clevers, V. Brunton, D. J. Winton, X. Wang, R. C. Sears, A. R. Clarke, M. C. Frame, O. J. Sansom, Focal adhesion kinase is required for intestinal regeneration and tumorigenesis downstream of Wnt/c-Myc signaling. *Dev Cell* **19**, 259-269 (2010).
8. J. K. Slack-Davis, E. D. Hershey, D. Theodorescu, H. F. Frierson, J. T. Parsons, Differential requirement for focal adhesion kinase signaling in cancer progression in the transgenic adenocarcinoma of mouse prostate model. *Mol Cancer Ther* **8**, 2470-2477 (2009).
9. A. Serrels, T. Lund, B. Serrels, A. Byron, R. C. McPherson, A. von Kriegsheim, L. Gomez-Cuadrado, M. Canel, M. Muir, J. E. Ring, E. Maniati, A. H. Sims, J. A. Pachter, V. G. Brunton, N. Gilbert, S. M. Anderton, R. J. Nibbs, M. C. Frame, Nuclear FAK controls chemokine transcription, Tregs, and evasion of anti-tumor immunity. *Cell* **163**, 160-173 (2015).
10. A. C. Cardoso, A. H. Pereira, A. L. Ambrosio, S. R. Consonni, R. Rocha de Oliveira, M. C. Bajgelman, S. M. Dias, K. G. Franchini, FAK Forms a Complex with MEF2 to Couple Biomechanical Signaling to Transcription in Cardiomyocytes. *Structure* **24**, 1301-1310 (2016).
11. S. T. Lim, N. L. Miller, X. L. Chen, I. Tancioni, C. T. Walsh, C. Lawson, S. Uryu, S. M. Weis, D. A. Cheresh, D. D. Schlaepfer, Nuclear-localized focal adhesion kinase regulates inflammatory VCAM-1 expression. *J Cell Biol* **197**, 907-919 (2012).
12. A. Serrels, K. McLeod, M. Canel, A. Kinnaird, K. Graham, M. C. Frame, V. G. Brunton, The role of focal adhesion kinase catalytic activity on the proliferation and migration of squamous cell carcinoma cells. *Int J Cancer* **131**, 287-297 (2012).
13. M. Milovanovic, V. Volarevic, G. Radosavljevic, I. Jovanovic, N. Pejnovic, N. Arsenijevic, M. L. Lukic, IL-33/ST2 axis in inflammation and immunopathology. *Immunol Res* **52**, 89-99 (2012).

14. X. Gao, X. Wang, Q. Yang, X. Zhao, W. Wen, G. Li, J. Lu, W. Qin, Y. Qi, F. Xie, J. Jiang, C. Wu, X. Zhang, X. Chen, H. Turnquist, Y. Zhu, B. Lu, Tumoral expression of IL-33 inhibits tumor growth and modifies the tumor microenvironment through CD8+ T and NK cells. *J Immunol* **194**, 438-445 (2015).
15. Y. Zhang, C. Davis, S. Shah, D. Hughes, J. C. Ryan, D. Altomare, M. M. Pena, IL-33 promotes growth and liver metastasis of colorectal cancer in mice by remodeling the tumor microenvironment and inducing angiogenesis. *Mol Carcinog* **56**, 272-287 (2017).
16. S. Ali, A. Mohs, M. Thomas, J. Klare, R. Ross, M. L. Schmitz, M. U. Martin, The dual function cytokine IL-33 interacts with the transcription factor NF-kappaB to dampen NF-kappaB-stimulated gene transcription. *J Immunol* **187**, 1609-1616 (2011).
17. Y. S. Choi, J. A. Park, J. Kim, S. S. Rho, H. Park, Y. M. Kim, Y. G. Kwon, Nuclear IL-33 is a transcriptional regulator of NF-kappaB p65 and induces endothelial cell activation. *Biochem Biophys Res Commun* **421**, 305-311 (2012).
18. Q. Yang, G. Li, Y. Zhu, L. Liu, E. Chen, H. Turnquist, X. Zhang, O. J. Finn, X. Chen, B. Lu, IL-33 synergizes with TCR and IL-12 signaling to promote the effector function of CD8+ T cells. *Eur J Immunol* **41**, 3351-3360 (2011).
19. D. P. Lu, X. Y. Zhou, L. T. Yao, C. G. Liu, W. Ma, F. Jin, Y. F. Wu, Serum soluble ST2 is associated with ER-positive breast cancer. *BMC Cancer* **14**, 198 (2014).
20. D. O. Villarreal, D. B. Weiner, Interleukin 33: a switch-hitting cytokine. *Curr Opin Immunol* **28**, 102-106 (2014).
21. A. A. Chackerian, E. R. Oldham, E. E. Murphy, J. Schmitz, S. Pflanz, R. A. Kastelein, IL-1 receptor accessory protein and ST2 comprise the IL-33 receptor complex. *J Immunol* **179**, 2551-2555 (2007).
22. A. Schmieder, G. Multhoff, J. Radons, Interleukin-33 acts as a pro-inflammatory cytokine and modulates its receptor gene expression in highly metastatic human pancreatic carcinoma cells. *Cytokine* **60**, 514-521 (2012).
23. D. Shao, F. Perros, G. Caramori, C. Meng, P. Dormuller, P. C. Chou, C. Church, A. Papi, P. Casolari, D. Welsh, A. Peacock, M. Humbert, I. M. Adcock, S. J. Wort, Nuclear IL-33 regulates soluble ST2 receptor and IL-6 expression in primary human arterial endothelial cells and is decreased in idiopathic pulmonary arterial hypertension. *Biochem Biophys Res Commun* **451**, 8-14 (2014).
24. M. Canel, A. Byron, A. H. Sims, J. Cartier, H. Patel, M. C. Frame, V. G. Brunton, B. Serrels, A. Serrels, Nuclear FAK and Runx1 cooperate to regulate IGFBP3, cell cycle progression and tumor growth. *Cancer Res*, (2017).
25. C. Schiering, T. Krausgruber, A. Chomka, A. Frohlich, K. Adelmann, E. A. Wohlfert, J. Pott, T. Griseri, J. Bollrath, A. N. Hegazy, O. J. Harrison, B. M. Owens, M. Lohning, Y. Belkaid, P. G. Fallon, F. Powrie, The alarmin IL-33 promotes regulatory T-cell function in the intestine. *Nature* **513**, 564-568 (2014).
26. L. Roussel, M. Erard, C. Cayrol, J. P. Girard, Molecular mimicry between IL-33 and KSHV for attachment to chromatin through the H2A-H2B acidic pocket. *EMBO Rep* **9**, 1006-1012 (2008).
27. K. J. Roux, D. I. Kim, M. Raida, B. Burke, A promiscuous biotin ligase fusion protein identifies proximal and interacting proteins in mammalian cells. *J Cell Biol* **196**, 801-810 (2012).
28. J. H. Lee, J. You, E. Dobrota, D. G. Skalnik, Identification and characterization of a novel human PP1 phosphatase complex. *J Biol Chem* **285**, 24466-24476 (2010).

29. J. H. Lee, D. G. Skalnik, Wdr82 is a C-terminal domain-binding protein that recruits the Setd1A Histone H3-Lys4 methyltransferase complex to transcription start sites of transcribed human genes. *Mol Cell Biol* **28**, 609-618 (2008).
30. J. Shi, W. A. Whyte, C. J. Zepeda-Mendoza, J. P. Milazzo, C. Shen, J. S. Roe, J. L. Minder, F. Mercan, E. Wang, M. A. Eckersley-Maslin, A. E. Campbell, S. Kawaoka, S. Shareef, Z. Zhu, J. Kendall, M. Muhar, C. Haslinger, M. Yu, R. G. Roeder, M. H. Wigler, G. A. Blobel, J. Zuber, D. L. Spector, R. A. Young, C. R. Vakoc, Role of SWI/SNF in acute leukemia maintenance and enhancer-mediated Myc regulation. *Genes Dev* **27**, 2648-2662 (2013).
31. S. Mujtaba, L. Zeng, M. M. Zhou, Structure and acetyl-lysine recognition of the bromodomain. *Oncogene* **26**, 5521-5527 (2007).
32. B. Huang, X. D. Yang, M. M. Zhou, K. Ozato, L. F. Chen, Brd4 coactivates transcriptional activation of NF-kappaB via specific binding to acetylated RelA. *Mol Cell Biol* **29**, 1375-1387 (2009).
33. B. P. Ashburner, S. D. Westerheide, A. S. Baldwin, Jr., The p65 (RelA) subunit of NF-kappaB interacts with the histone deacetylase (HDAC) corepressors HDAC1 and HDAC2 to negatively regulate gene expression. *Mol Cell Biol* **21**, 7065-7077 (2001).
34. S. T. Lim, X. L. Chen, Y. Lim, D. A. Hanson, T. T. Vo, K. Howerton, N. Larocque, S. J. Fisher, D. D. Schlaepfer, D. Ilic, Nuclear FAK promotes cell proliferation and survival through FERM-enhanced p53 degradation. *Mol Cell* **29**, 9-22 (2008).
35. E. Lefrancais, C. Cayrol, Mechanisms of IL-33 processing and secretion: differences and similarities between IL-1 family members. *Eur Cytokine Netw* **23**, 120-127 (2012).
36. M. Wu, P. F. Wang, J. S. Lee, S. Martin-Brown, L. Florens, M. Washburn, A. Shilatifard, Molecular regulation of H3K4 trimethylation by Wdr82, a component of human Set1/COMPASS. *Mol Cell Biol* **28**, 7337-7344 (2008).
37. Z. Zou, B. Huang, X. Wu, H. Zhang, J. Qi, J. Bradner, S. Nair, L. F. Chen, Brd4 maintains constitutively active NF-kappaB in cancer cells by binding to acetylated RelA. *Oncogene* **33**, 2395-2404 (2014).
38. B. Turriziani, A. Garcia-Munoz, R. Pilkington, C. Raso, W. Kolch, A. von Kriegsheim, On-beads digestion in conjunction with data-dependent mass spectrometry: a shortcut to quantitative and dynamic interaction proteomics. *Biology (Basel)* **3**, 320-332 (2014).
39. J. A. Vizcaino, A. Csordas, N. Del-Toro, J. A. Dianes, J. Griss, I. Lavidas, G. Mayer, Y. Perez-Riverol, F. Reisinger, T. Ternent, Q. W. Xu, R. Wang, H. Hermjakob, 2016 update of the PRIDE database and its related tools. *Nucleic Acids Res* **44**, 11033 (2016).
40. W. Huang da, B. T. Sherman, R. A. Lempicki, Bioinformatics enrichment tools: paths toward the comprehensive functional analysis of large gene lists. *Nucleic Acids Res* **37**, 1-13 (2009).
41. P. Shannon, A. Markiel, O. Ozier, N. S. Baliga, J. T. Wang, D. Ramage, N. Amin, B. Schwikowski, T. Ideker, Cytoscape: a software environment for integrated models of biomolecular interaction networks. *Genome Res* **13**, 2498-2504 (2003).
42. M. J. de Hoon, S. Imoto, J. Nolan, S. Miyano, Open source clustering software. *Bioinformatics* **20**, 1453-1454 (2004).
43. A. J. Saldanha, Java Treeview--extensible visualization of microarray data. *Bioinformatics* **20**, 3246-3248 (2004).

44. A. I. Saeed, V. Sharov, J. White, J. Li, W. Liang, N. Bhagabati, J. Braisted, M. Klapa, T. Currier, M. Thiagarajan, A. Sturn, M. Snuffin, A. Rezantsev, D. Popov, A. Ryltsov, E. Kostukovich, I. Borisovsky, Z. Liu, A. Vinsavich, V. Trush, J. Quackenbush, TM4: a free, open-source system for microarray data management and analysis. *Biotechniques* **34**, 374-378 (2003).

Acknowledgments: We would like to thank the FACS facility at the MRC-Centre for Inflammation Research, University of Edinburgh for their help with FACS analysis, and the CBS animal technicians at LF2, University of Edinburgh for their assistance with biological work.

Funding: This work was supported by Cancer Research UK (Grant no. C157/A15703 to M.C.F.), European Research Council (Grant no. 299440 Cancer Innovation to M.C.F.). A.v.K. is supported by the Cancer Research UK Edinburgh centre grant. N.Q is supported by the Welcome Trust-UoE ISSF2 programme. D.T. is supported by Cancer Research UK (Grant no. C54352/A22011 awarded to S.M.A.).

Author contributions: B.S., A.S., and M.C.F. devised and oversaw the project. B.S., A.S., N.M., A.B., S.M.A., and M.C.F. designed the experiments with contributions from M.C. and H.M. B.S., A.S., N.M., M.C., A.B., S.C.J., N.Q. D.T., performed the experiments with contributions from A.v.K., and B.S., A.S., N.M., M.C., A.B., N.Q., S.C.J., analysed the data. B.S., and A.B., performed bioinformatics analysis. B.S., A.S., and M.C.F., wrote the manuscript with contributions from A.B., and N.M.; all authors commented on and approved the final version.

Competing interests: The authors declare that they have no competing interests.

Data and materials availability: The mass spectrometery proteomics data have been deposited to the ProteomeXchange Consortium via the PRIDE partner repository, dataset identifier PXD007698.

Figure Legends

Figure 1. Nuclear FAK regulates expression of IL33 and its receptor ST2. (A) Gene ontology enrichment analysis (cellular component terms) on the significantly down-regulated set of genes in the *FAK*$^{-/-}$ SCC transcriptome relative to the wild-type (wt) (predicated false positives *(pfp)*< 0.05). Genes annotated with the overrepresented term (extracellular region; Benjamini–Hochberg-corrected hypergeometric test) were used to seed a protein interaction network based on direct physical interactions (grey lines). Color of each node (circle) is proportional to the log-transformed fold change in gene expression. The largest connected graph component is displayed. **(B and C)** Abundance of IL33 at the mRNA level (B; by qRT-PCR) and protein level (C; by Western blot) in FAK-wt, *FAK*$^{-/-}$, FAK-nls, and FAK-kd SCC cells. **(D and E)** Abundance of *IL33* mRNA (D; by qRT-PCR) and IL33 protein (E; by Western blot) in FAK-wt SCC cells treated with control (DMSO) or VS4718 (250 nM, 24 hours). Western blot additionally assessed in *FAK*$^{-/-}$ SCC cells for reference. **(F)** Analysis of ELISA for IL33 in conditioned media from FAK-wt, *FAK*$^{-/-}$, FAK-nls, and FAK-kd SCC cells. **(G)** qRT-PCR analysis of *ST2* expression in FAK-wt, *FAK*$^{-/-}$, FAK-nls, and FAK-kd SCC cells. **(H)** Analysis of ELISA for sST2 in conditioned media from FAK-wt, *FAK*$^{-/-}$, FAK-nls, and FAK-kd SCC cells. **(I)** qRT-PCR analysis of *ST2* expression in FAK-wt SCC cells treated with control (DMSO) or VS4718 (250 nM, 24 hours). **(J)** Analysis of ELISA for sST2 in conditioned media from FAK-wt SCC cells treated with control (DMSO) or VS4718 (250 nM, 24 hours). Data are mean ± S.E.M. n=3 experiments. *p ≤ 0.05, **p ≤ 0.01, ***p ≤ 0.001, ****p ≤ 0.0001; by Tukey corrected one-way ANOVA (B, G and H) or two-tailed unpaired *t*-test (D, I, and J).

Figure 2. Nuclear FAK and IL33 cooperate to regulate chemokine expression. **(A)** Representative Western blot of IL33 abundance in FAK-wt, FAK-wt pLKO, and FAK-wt IL33 shRNA1 SCC cells. **(B)** qRT-PCR analysis of *IL33* expression in FAK-wt pLKO, *FAK*$^{-/-}$, and FAK-wt IL33-shRNA1 SCC cells. **(C and D)** qRT-PCR analysis of *IL33* (C) and *Ccl5* (D) expression in primary keratinocytes and FAK-wt SCC cells. **(E)** qRT-PCR analysis of *Ccl5* expression in FAK-wt pLKO, *FAK*$^{-/-}$, and FAK-wt IL33-shRNA1 cells. **(F)** NanoString analysis of chemokine expression in FAK-wt pLKO, *FAK*$^{-/-}$ and FAK-wt IL33-shRNA1 SCC cells. Log_{10}-transformed expression levels for chemokines with at least 50 counts were hierarchically clustered and displayed as a heatmap. Pearson correlation coefficient between expression profiles in *FAK*$^{-/-}$ and FAK-wt IL33-shRNA1 SCC cells is shown. Log_2-transformed fold changes (over SCC FAK-wt pLKO) are also displayed. **(G)** qRT-PCR analysis of *Ccl5* expression in SCC *FAK*$^{-/-}$ and *FAK*$^{-/-}$+IL33 cells. Data are mean ± S.E.M. n = 3 for all experiments. *p≤ 0.05, **p ≤ 0.01,***p ≤ 0.001, ****p ≤ 0.0001; by Tukey corrected one-way ANOVA (B and E) or two-tailed unpaired t-test (C, D and G).

Figure 3. IL33 and sST2 support SCC tumour growth through suppressing the anti-tumour immune response. (A and B) Representative growth of FAK-wt, *FAK*$^{-/-}$, and FAK-wt IL33-shRNA1 (A) or FAK-wt IL33-CRISPR (B) SCC tumors after orthotopic subcutaneous implantation. **(C)** qRT-PCR analysis of *ST2* expression in FAK-wt pLKO, FAK-wt ST2-shRNA1, and FAK-wt ST2-shRNA2 SCC cells. **(D)** Growth of FAK-wt ST2-shRNA (pools 1 and 2) SCC tumors after orthotopic subcutaneous implantation. **(E)** $CD45^+$ cells as a percentage of live cells isolated from FAK-wt SCC tumors 12 days after implantation. **(F)** Abundance of different immune cell populations as a percentage of $CD45^+$ cells. Marker sets used to identify cell populations are listed

in fig. S3. **(G)** Percentage $ST2^+$ cells in different immune cell populations. **(H)** Mean fluorescent intensity of ST2 expression in different immune cell populations. **(I)** Representative growth of FAK-wt, FAK-wt ST2-shRNA1, and FAK-wt ST2-shRNA2 SCC tumors receiving treatment with either a CD8-depleting antibody or isotype control antibody. Statistics in C, ****p ≤ 0.0001 by Tukey corrected one-way ANOVA. Data are mean ± S.E.M, n = 3 for q(RT)-PCR, n = 6-8 tumors.

Figure 4. Nuclear IL33 interacts with an extensive network of transcriptional regulators. (A) Representative Western blot of IL33 abundance in cytoplasmic (cyto), nuclear (Nuc), and chromatin (Chr) fractions from FAK-wt and *FAK*$^{-/-}$ SCC cells. **(B)** Representative Western blot of IL33 abundance in FAK-wt IL33-CRISPR/BirA-E.V. and FAK-wt IL33-CRISPR/IL33-BirA SCC cells. **(C)** Western blot analysis of lysates from nuclear fractionations of IL33-BirA fusion protein expression in FAK-wt IL33-CRISPR/E.V. or FAK-wt IL33-CRISPR/IL33-BirA SCC cells. **(D)** Functional interaction network analysis of the IL33 interactome. Direct physical interactions (solid grey lines) and functional association with transcription (dashed grey lines) are shown. Node style indicates association with additional relevant overrepresented functions (p<0.0001, Benjamini–Hochberg-corrected hypergeometric test). Components of the PTW/PP1 phosphatase, Baf-type and TFIID complexes are highlighted. **(E)** Western blot analysis of key network components using streptavidin pulldowns from biotinylated lysates of SCC FAK-wt IL33 CRISPR cells expressing either BirA empty vector or IL33-BirA fusion protein. **(F)** Representative Western blot of chromatin fractions and whole cell lysates from SCC FAK-wt, FAK-wt pLKO, and FAK-wt IL33 shRNA1 cells. **(G)** Interrogation of the IL33 BioID protein interaction network to identify potential upstream regulators of m*Ccl5* promoter associated transcription factors (taken from

Qiagen ENCODE database). PP, protein-protein interaction; E, expression; PD, protein-DNA interaction; T, transactivation; A, activation. **(H)** Western blot analysis of IL33:BRD4, IL33:FAK, and IL33:HDAC1 associations using streptavidin pulldowns from biotinylated lysates of FAK-wt IL33-CRISPR SCC cells expressing either BirA empty vector or IL33-BirA fusion protein. **(I)** qRT-PCR analysis of *Ccl5* expression in SCC FAK-wt cells treated with DMSO or JQ1 (200nM for 48 hours). **(J)** q(RT)-PCR analysis of Ccl5 expression in FAK-wt SCC cells treated with DMSO or vorinostat (10μM for 24 hours). Statistics in I and J, ****p ≤ 0.0001, ***p ≤ 0.001, ** ≤ 0.01. Two-tailed unpaired t-test. n = 3 for all experiments.

Figure 5. Nuclear FAK regulates IL33/ST2 signaling to control the anti-tumor immune response. Model of the mechanism. Nuclear FAK regulates *IL33* expression ("1") through interaction with transcription factors (TF) and transcriptional regulators (TR). Nuclear FAK and IL33 cooperate to drive expression of *Ccl5* and *sST2* ("2" and "3", respectively) through interaction with TFs and TRs. Ccl5 and sST2 are secreted from SCC cancer cells, promoting immune evasion. We have previously reported a CCL5-CCR1,3, and 5 paracrine signaling axis between FAK-wt SCC cells and tumor-infiltrating T_{reg} cells that contributes to immune evasion. We propose that sST2 contributes to immune evasion through competitive inhibition of IL33/ST2 signaling on cytotoxic $CD8^+$ T-cells ("4"), resulting in tumor tolerance.

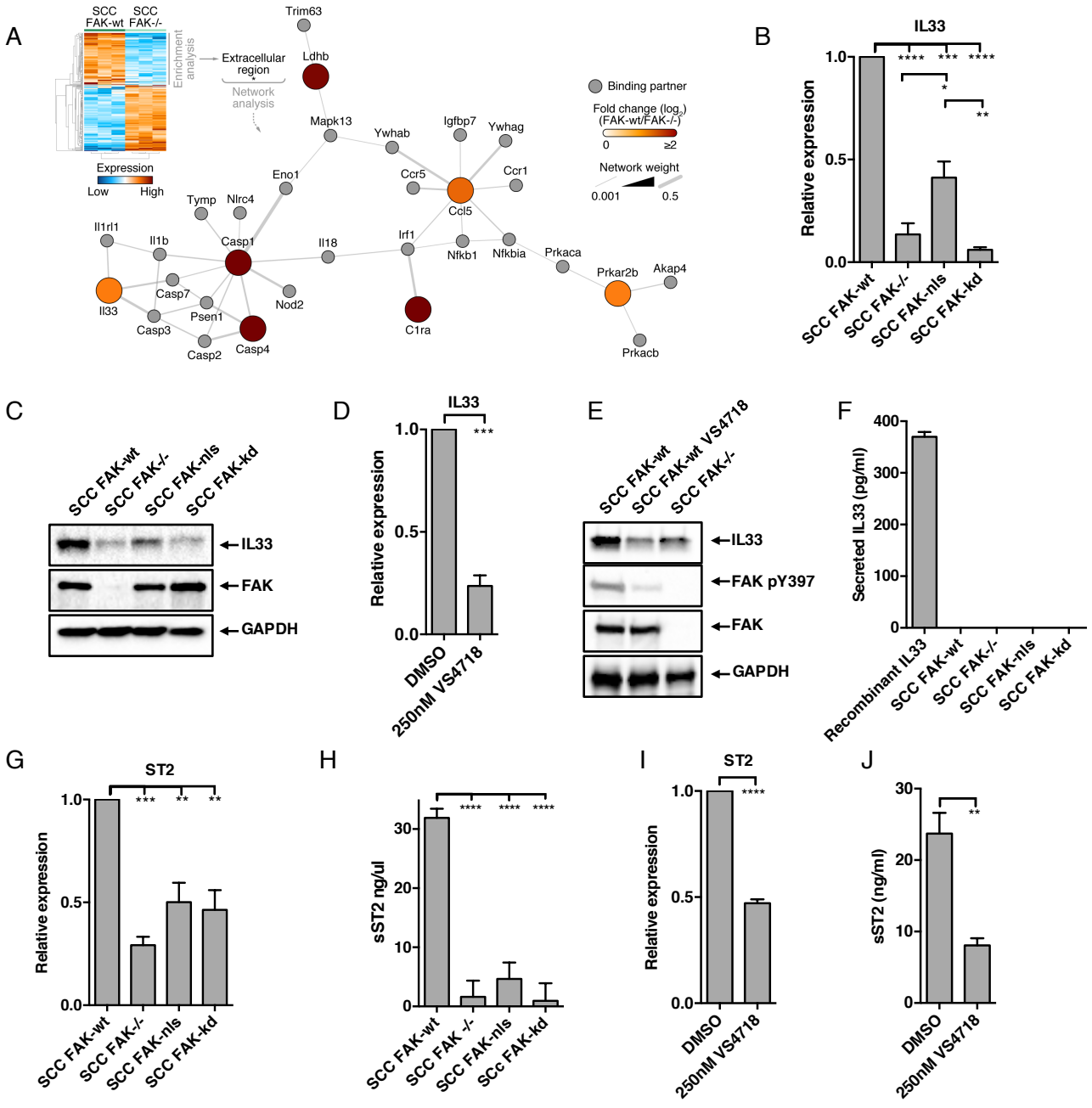
A
SCC FAK-wt
SCC FAK-/-
Enrichment analysis
Extracellular region
Network analysis
Expression
Low
High
Trim63
Ldhb
Mapk13
Ywhab
Igfbp7
Ywhag
Ccr5
Ccr1
Ccl5
Eno1
Tymp
Nlrc4
Casp1
Il1rl1
Il1b
Il18
Irf1
Nfkb1
Nfkbia
Prkaca
Prkar2b
Akap4
Il33
Casp7
Nod2
Psen1
Casp3
Casp2
Casp4
C1ra
Prkacb
Binding partner
Fold change (log2) (FAK-wt/FAK-/-)
0
≥2
Network weight
0.001
0.5
B
IL33
Relative expression
SCC FAK-wt
SCC FAK-/-
SCC FAK-nls
SCC FAK-kd
C
SCC FAK-wt
SCC FAK-/-
SCC FAK-nls
SCC FAK-kd
IL33
FAK
GAPDH
D
IL33
Relative expression
DMSO
250nM VS4718
E
SCC FAK-wt
SCC FAK-wt VS4718
SCC FAK-/-
IL33
FAK pY397
FAK
GAPDH
F
Secreted IL33 (pg/ml)
Recombinant IL33
SCC FAK-wt
SCC FAK-/-
SCC FAK-nls
SCC FAK-kd
G
ST2
Relative expression
SCC FAK-wt
SCC FAK-/-
SCC FAK-nls
SCC FAK-kd
H
sST2 ng/ul
SCC FAK-wt
SCC FAK -/-
SCC FAK-nls
SCc FAK-kd
I
ST2
Relative expression
DMSO
250nM VS4718
J
sST2 (ng/ml)
DMSO
250nM VS4718

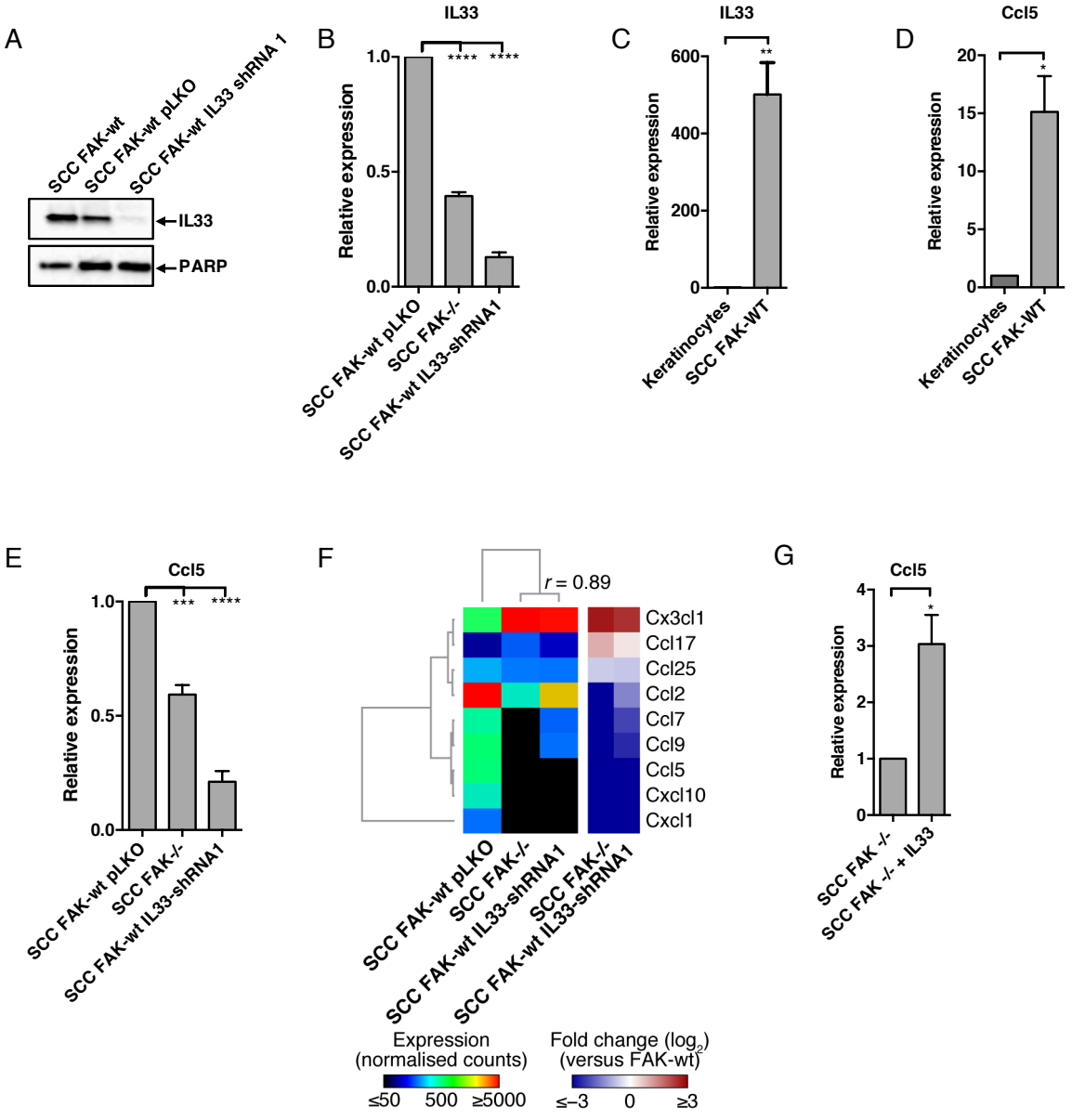
A
SCC FAK-wt
SCC FAK-wt pLKO
SCC FAK-wt IL33 shRNA 1
IL33
PARP
B
IL33
Relative expression
1.0
0.5
0.0
****
****
SCC FAK-wt pLKO
SCC FAK-/-
SCC FAK-wt IL33-shRNA1
C
IL33
Relative expression
600
400
200
0
**
Keratinocytes
SCC FAK-WT
D
Ccl5
Relative expression
20
15
10
5
0
*
Keratinocytes
SCC FAK-WT
E
Ccl5
Relative expression
1.0
0.5
0.0
***
****
SCC FAK-wt pLKO
SCC FAK-/-
SCC FAK-wt IL33-shRNA1
F
r = 0.89
Cx3cl1
Ccl17
Ccl25
Ccl2
Ccl7
Ccl9
Ccl5
Cxcl10
Cxcl1
SCC FAK-wt pLKO
SCC FAK-/-
SCC FAK-wt IL33-shRNA1
SCC FAK-/-
SCC FAK-wt IL33-shRNA1
Expression
(normalised counts)
≤50
500
≥5000
Fold change (log2)
(versus FAK-wt)
≤–3
0
≥3
G
Ccl5
Relative expression
4
3
2
1
0
*
SCC FAK -/-
SCC FAK -/- + IL33

Figure 2

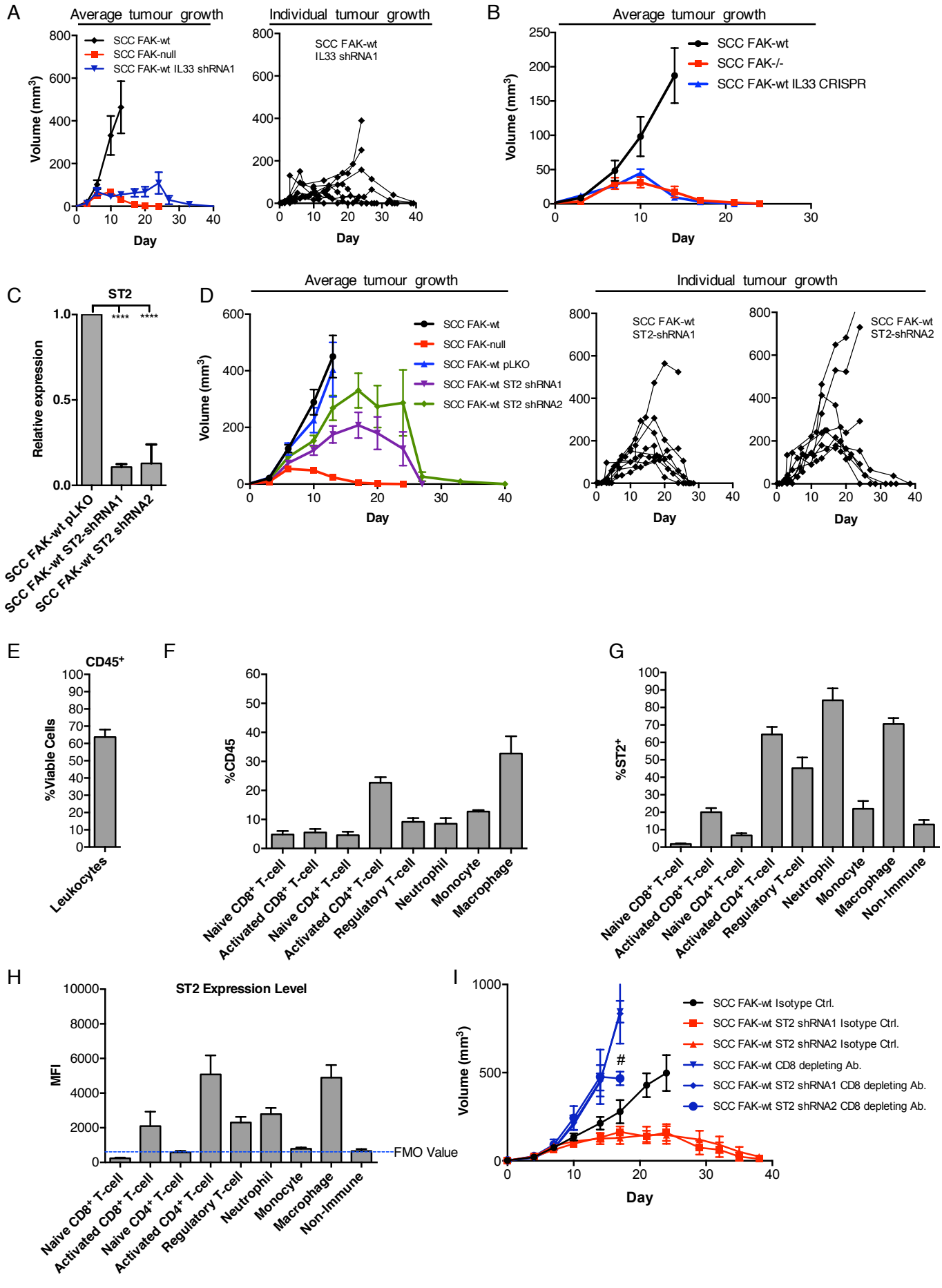
A
Average tumour growth
Individual tumour growth
SCC FAK-wt
SCC FAK-null
SCC FAK-wt IL33 shRNA1
SCC FAK-wt IL33 shRNA1
Volume (mm3)
Day
B
Average tumour growth
SCC FAK-wt
SCC FAK-/-
SCC FAK-wt IL33 CRISPR
Volume (mm3)
Day
C
ST2
Relative expression
****
****
SCC FAK-wt pLKO
SCC FAK-wt ST2-shRNA1
SCC FAK-wt ST2 shRNA2
D
Average tumour growth
Individual tumour growth
SCC FAK-wt
SCC FAK-null
SCC FAK-wt pLKO
SCC FAK-wt ST2 shRNA1
SCC FAK-wt ST2 shRNA2
SCC FAK-wt ST2-shRNA1
SCC FAK-wt ST2-shRNA2
Volume (mm3)
Day
E
CD45+
%Viable Cells
Leukocytes
F
%CD45
Naive CD8+ T-cell
Activated CD8+ T-cell
Naive CD4+ T-cell
Activated CD4+ T-cell
Regulatory T-cell
Neutrophil
Monocyte
Macrophage
G
%ST2+
Naive CD8+ T-cell
Activated CD8+ T-cell
Naive CD4+ T-cell
Activated CD4+ T-cell
Regulatory T-cell
Neutrophil
Monocyte
Macrophage
Non-Immune
H
ST2 Expression Level
MFI
FMO Value
Naive CD8+ T-cell
Activated CD8+ T-cell
Naive CD4+ T-cell
Activated CD4+ T-cell
Regulatory T-cell
Neutrophil
Monocyte
Macrophage
Non-Immune
I
SCC FAK-wt Isotype Ctrl.
SCC FAK-wt ST2 shRNA1 Isotype Ctrl.
SCC FAK-wt ST2 shRNA2 Isotype Ctrl.
SCC FAK-wt CD8 depleting Ab.
SCC FAK-wt ST2 shRNA1 CD8 depleting Ab.
SCC FAK-wt ST2 shRNA2 CD8 depleting Ab.
#
Volume (mm3)
Day

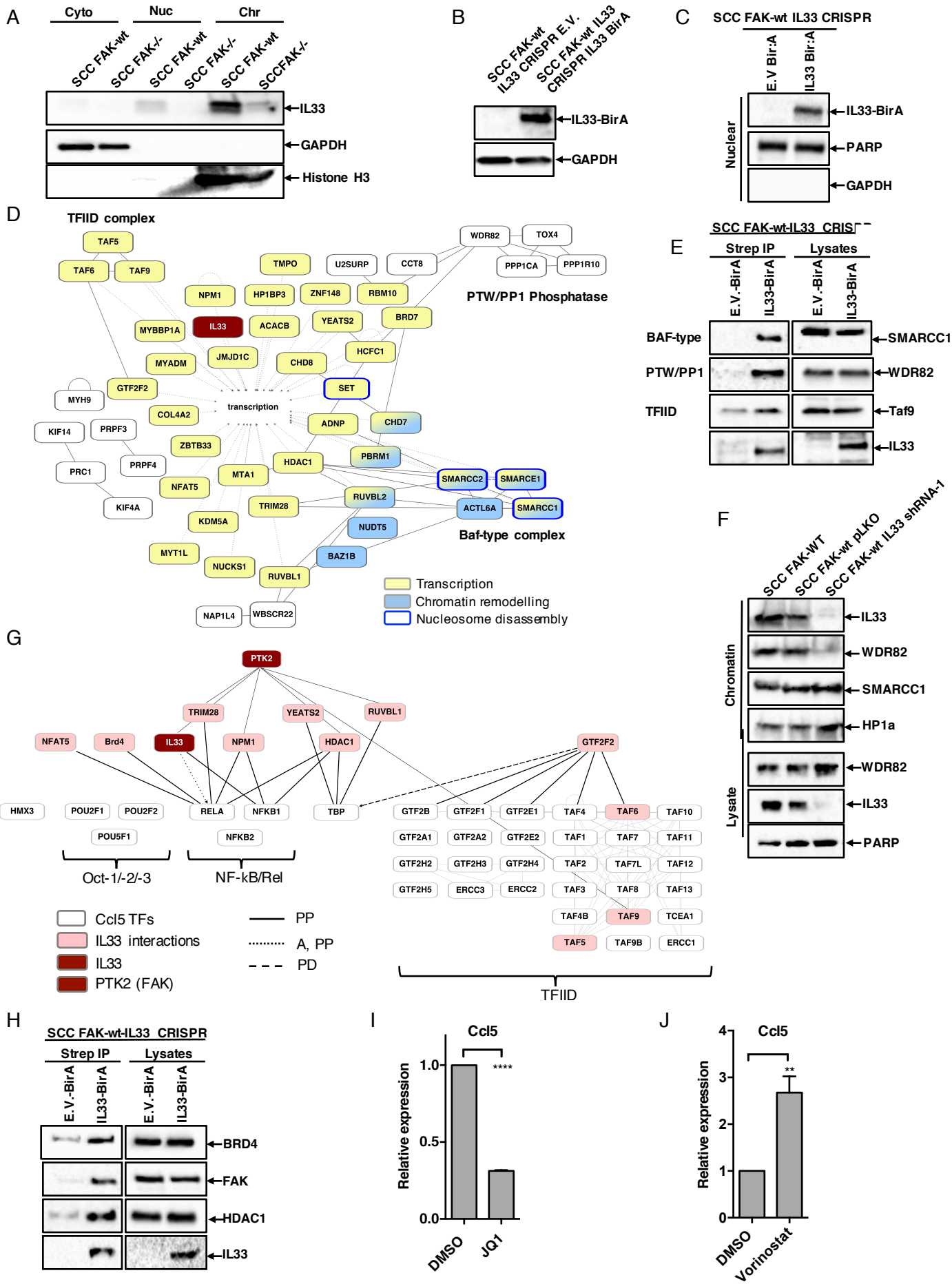
A
Cyto
Nuc
Chr
SCC FAK-wt
SCC FAK-/-
SCC FAK-wt
SCC FAK-/-
SCC FAK-wt
SCCFAK-/-
IL33
GAPDH
Histone H3
B
SCC FAK-wt IL33 CRISPR E.V.
SCC FAK-wt IL33 CRISPR IL33 BirA
IL33-BirA
GAPDH
C
SCC FAK-wt IL33 CRISPR
E.V Bir:A
IL33 Bir:A
Nuclear
IL33-BirA
PARP
GAPDH
D
TFIID complex
TAF5
TAF6
TAF9
TMPO
U2SURP
CCT8
WDR82
TOX4
PPP1CA
PPP1R10
PTW/PP1 Phosphatase
NPM1
HP1BP3
ZNF148
RBM10
BRD7
MYBBP1A
IL33
ACACB
YEATS2
HCFC1
MYADM
JMJD1C
CHD8
GTF2F2
SET
MYH9
transcription
COL4A2
ADNP
CHD7
KIF14
PRPF3
ZBTB33
PBRM1
PRC1
PRPF4
HDAC1
MTA1
SMARCC2
SMARCE1
NFAT5
RUVBL2
TRIM28
ACTL6A
SMARCC1
KIF4A
KDM5A
NUDT5
Baf-type complex
MYT1L
BAZ1B
NUCKS1
RUVBL1
NAP1L4
WBSCR22
Transcription
Chromatin remodelling
Nucleosome disassembly
E
SCC FAK-wt-IL33 CRIS
Strep IP
Lysates
E.V.-BirA
IL33-BirA
E.V.-BirA
IL33-BirA
BAF-type
SMARCC1
PTW/PP1
WDR82
TFIID
Taf9
IL33
F
SCC FAK-WT
SCC FAK-wt pLKO
SCC FAK-wt IL33 shRNA-1
Chromatin
IL33
WDR82
SMARCC1
HP1a
Lysate
WDR82
IL33
PARP
G
PTK2
TRIM28
YEATS2
RUVBL1
NFAT5
Brd4
IL33
NPM1
HDAC1
GTF2F2
HMX3
POU2F1
POU2F2
RELA
NFKB1
TBP
GTF2B
GTF2F1
GTF2E1
TAF4
TAF6
TAF10
POU5F1
NFKB2
GTF2A1
GTF2A2
GTF2E2
TAF1
TAF7
TAF11
GTF2H2
GTF2H3
GTF2H4
TAF2
TAF7L
TAF12
GTF2H5
ERCC3
ERCC2
TAF3
TAF8
TAF13
TAF4B
TAF9
TCEA1
TAF5
TAF9B
ERCC1
Oct-1/-2/-3
NF-kB/Rel
TFIID
Ccl5 TFs
IL33 interactions
IL33
PTK2 (FAK)
PP
A, PP
PD
H
SCC FAK-wt-IL33 CRISPR
Strep IP
Lysates
E.V.-BirA
IL33-BirA
E.V.-BirA
IL33-BirA
BRD4
FAK
HDAC1
IL33
I
Ccl5
****
Relative expression
1.0
0.5
0.0
DMSO
JQ1
J
Ccl5
**
Relative expression
4
3
2
1
0
DMSO
Vorinostat

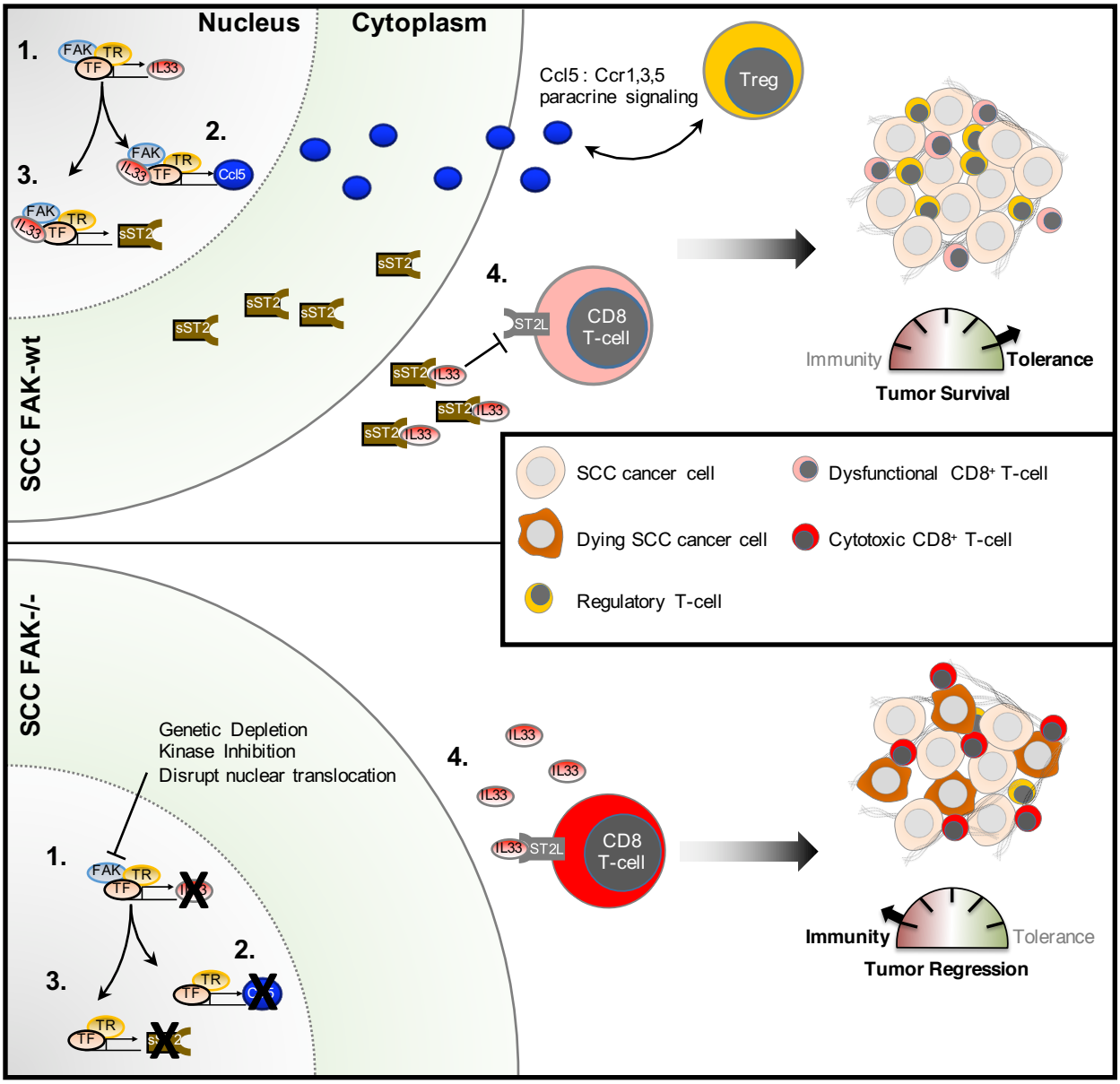
Nucleus
Cytoplasm
1.
FAK
TR
TF
IL33
2.
3.
Ccl5
sST2
4.
ST2L
CD8
T-cell
Ccl5 : Ccr1,3,5
paracrine signaling
Treg
Immunity
Tolerance
Tumor Survival
SCC FAK-wt
SCC cancer cell
Dysfunctional CD8+ T-cell
Dying SCC cancer cell
Cytotoxic CD8+ T-cell
Regulatory T-cell
SCC FAK-/-
Genetic Depletion
Kinase Inhibition
Disrupt nuclear translocation
Immunity
Tolerance
Tumor Regression

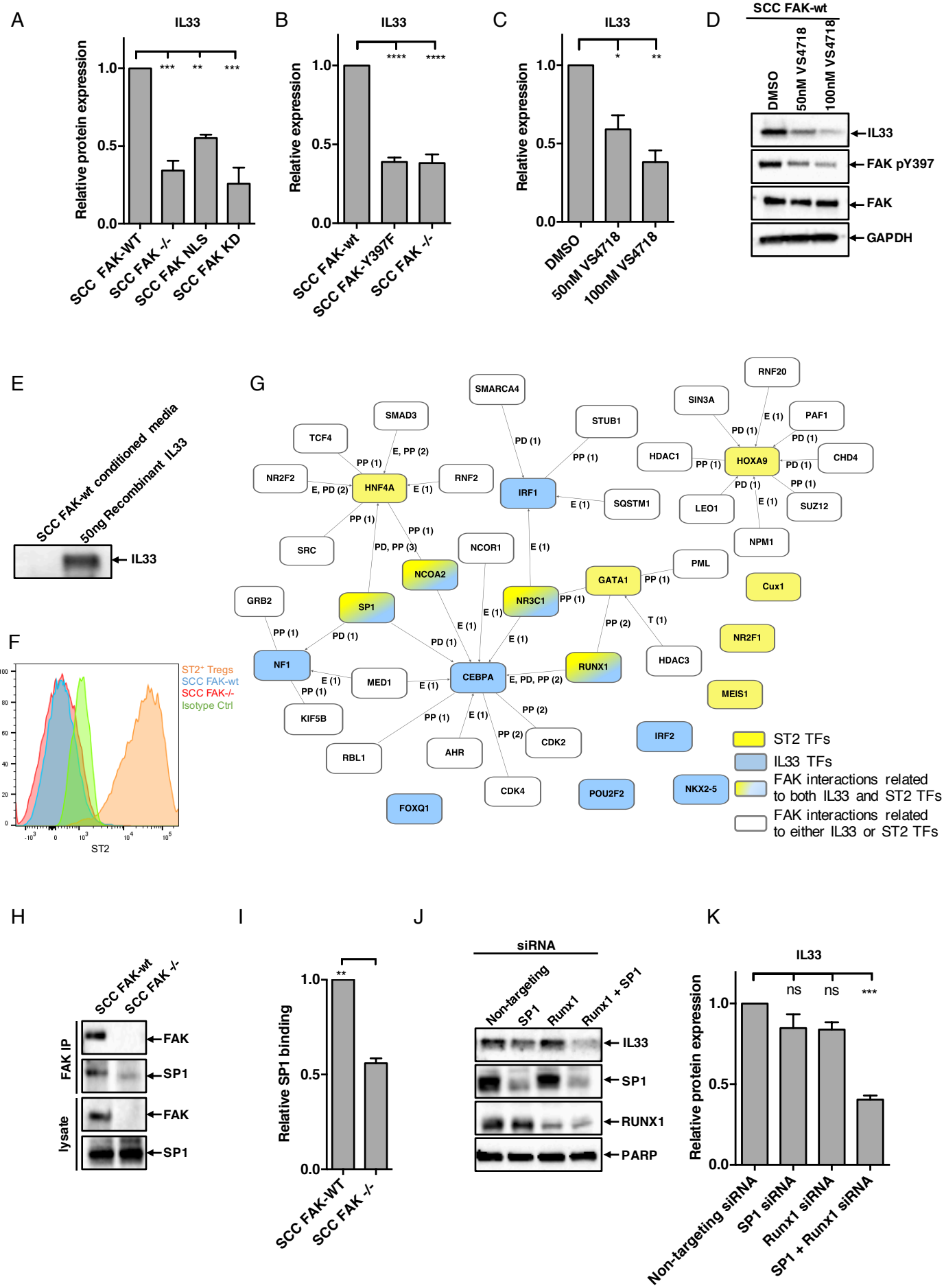
A
IL33
Relative protein expression
1.0
0.5
0.0
***
**
***
SCC FAK-WT
SCC FAK -/-
SCC FAK NLS
SCC FAK KD
B
IL33
Relative expression
1.0
0.5
0.0
****
****
SCC FAK-wt
SCC FAK-Y397F
SCC FAK -/-
C
IL33
Relative expression
1.0
0.5
0.0
*
**
DMSO
50nM VS4718
100nM VS4718
D
SCC FAK-wt
DMSO
50nM VS4718
100nM VS4718
IL33
FAK pY397
FAK
GAPDH
E
SCC FAK-wt conditioned media
50ng Recombinant IL33
IL33
F
ST2+ Tregs
SCC FAK-wt
SCC FAK-/-
Isotype Ctrl
100
80
60
40
20
0
-10^3
0
10^3
10^4
10^5
ST2
G
SMARCA4
RNF20
SIN3A
SMAD3
STUB1
PAF1
TCF4
HDAC1
HOXA9
CHD4
NR2F2
HNF4A
RNF2
IRF1
SQSTM1
LEO1
SUZ12
SRC
NCOR1
NPM1
NCOA2
PML
GATA1
Cux1
GRB2
SP1
NR3C1
NR2F1
NF1
MED1
CEBPA
RUNX1
HDAC3
MEIS1
KIF5B
IRF2
RBL1
AHR
CDK2
CDK4
POU2F2
NKX2-5
FOXQ1
PP (1)
PD (1)
E (1)
E, PP (2)
E, PD (2)
PD, PP (3)
T (1)
PP (2)
E, PD, PP (2)
ST2 TFs
IL33 TFs
FAK interactions related to both IL33 and ST2 TFs
FAK interactions related to either IL33 or ST2 TFs
H
SCC FAK-wt
SCC FAK -/-
FAK IP
FAK
SP1
lysate
FAK
SP1
I
Relative SP1 binding
1.0
0.5
0.0
**
SCC FAK-WT
SCC FAK -/-
J
siRNA
Non-targeting
SP1
Runx1
Runx1 + SP1
IL33
SP1
RUNX1
PARP
K
IL33
Relative protein expression
1.0
0.5
0.0
ns
ns
***
Non-targeting siRNA
SP1 siRNA
Runx1 siRNA
SP1 + Runx1 siRNA

A

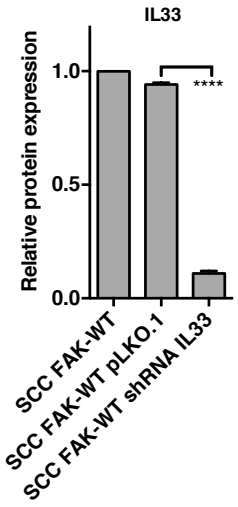
IL33
Relative protein expression
1.0
0.5
0.0
****
SCC FAK-WT
SCC FAK-WT pLKO.1
SCC FAK-WT shRNA IL33

B

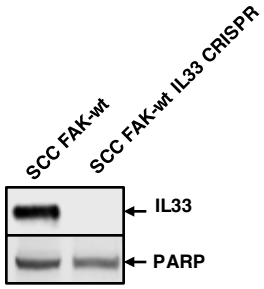
SCC FAK-wt
SCC FAK-wt IL33 CRISPR
IL33
PARP

C

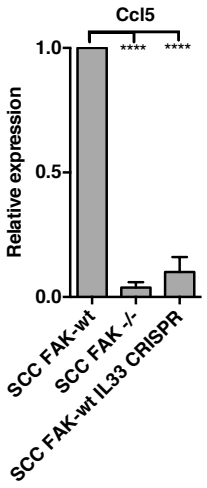
Ccl5
Relative expression
1.0
0.5
0.0
****
****
SCC FAK-wt
SCC FAK -/-
SCC FAK-wt IL33 CRISPR

D

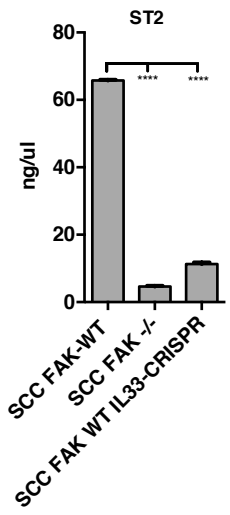
ST2
ng/ul
80
60
40
20
0
****
****
SCC FAK-WT
SCC FAK -/-
SCC FAK WT IL33-CRISPR

Naïve $CD8^+$ T-cell	$CD45^+CD3^+CD8^+CD44^-FoxP3^-$
Activated $CD8^+$ T-cell	$CD45^+CD3^+CD8^+CD44^+FoxP3^-$
Naïve $CD4^+$ T-cell	$CD45^+CD3^+CD8^-CD44^-FoxP3^-$
Activated $CD4^+$ T-cell	$CD45^+CD3^+CD8^-CD44^+FoxP3^-$
Regulatory T-cell	$CD45^+CD3^+CD8^-FoxP3^+$
Neutrophil	$CD45^+CD11b^+Ly6G^+$
Monocyte	$CD45^+CD11b^+Ly6G^-F480^-$
Macrophage	$CD45^+CD11b^+Ly6G^-F480^+$

A

GO Biological Processes	PValue	Benjamini
covalent chromatin modification	8.26E-12	5.91E-09
ATP-dependent chromatin remodeling	7.94E-09	2.84E-06
transcription, DNA-templated	2.00E-08	4.77E-06
chromatin remodeling	3.05E-08	5.45E-06
regulation of transcription, DNA-templated	5.58E-07	7.98E-05
circadian regulation of gene expression	3.76E-05	0.00447197
protein homotetramerization	9.55E-05	0.00971143
nucleosome assembly	4.71E-04	0.04121492

B

GO Cellular Component	PValue	Benjamini
nucleus	7.19E-17	2.59E-14
nucleoplasm	5.52E-16	6.46E-14
BAF-type complex	3.83E-08	2.98E-06
MLL1 complex	5.78E-07	3.37E-05
nuclear chromatin	1.01E-06	4.69E-05
stress fiber	2.76E-06	1.07E-04
cytoskeleton	7.52E-06	2.50E-04
chromatin	9.81E-06	2.86E-04
PTW/PP1 phosphatase complex	1.10E-05	2.84E-04
myosin complex	1.37E-05	3.18E-04
protein complex	2.01E-05	4.25E-04
npBAF complex	5.48E-05	0.00106371
SWI/SNF complex	5.48E-05	0.00106371
Cajal body	1.69E-04	0.00301872
U4/U6 x U5 tri-snRNP complex	3.70E-04	0.00613935
cytoplasm	4.17E-04	0.00645534
spindle	6.24E-04	0.00905423
actin cytoskeleton	0.00123789	0.01683361
actomyosin	0.00183305	0.02346974
cell-cell adherens junction	0.00271538	0.03279457
nBAF complex	0.00299798	0.03437421
transcription factor TFTC complex	0.00299798	0.03437421
microtubule	0.00328049	0.03580108
Ino80 complex	0.00344591	0.03589811
nucleolus	0.00409015	0.04066978
chromosome	0.00432565	0.04121259

C

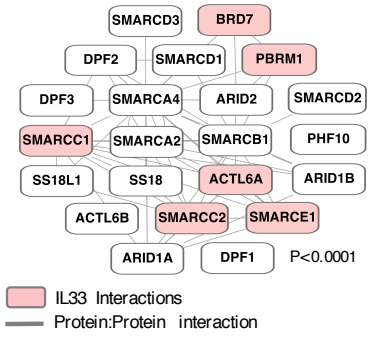

D

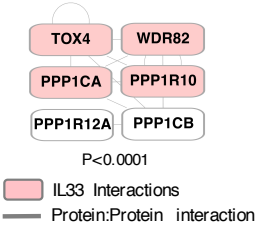

E

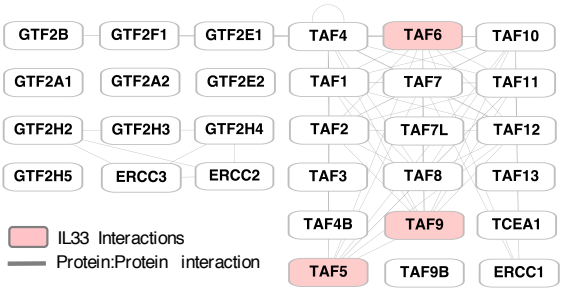

F

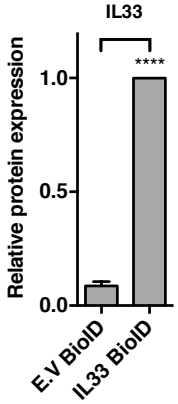

G

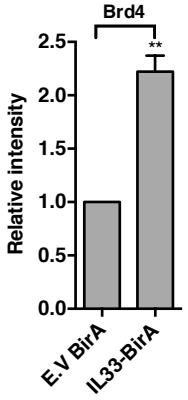

H